



**HAL**  
open science

# A comparative study of semiempirical, ab initio, and DFT methods in evaluating metal-ligand bond strength, proton affinity, and interactions between first and second shell ligands in Zn-biomimetic complexes

Gilles Frison, Gilles Ohanessian

► **To cite this version:**

Gilles Frison, Gilles Ohanessian. A comparative study of semiempirical, ab initio, and DFT methods in evaluating metal-ligand bond strength, proton affinity, and interactions between first and second shell ligands in Zn-biomimetic complexes. *Journal of Computational Chemistry*, 2008, 29, pp.416-433. 10.1002/jcc.20800 . hal-00466475

**HAL Id: hal-00466475**

**<https://hal.science/hal-00466475>**

Submitted on 23 Mar 2010

**HAL** is a multi-disciplinary open access archive for the deposit and dissemination of scientific research documents, whether they are published or not. The documents may come from teaching and research institutions in France or abroad, or from public or private research centers.

L'archive ouverte pluridisciplinaire **HAL**, est destinée au dépôt et à la diffusion de documents scientifiques de niveau recherche, publiés ou non, émanant des établissements d'enseignement et de recherche français ou étrangers, des laboratoires publics ou privés.

**A comparative study of semiempirical, *ab initio* and DFT methods in evaluating metal-ligand bond strength, proton affinity and interactions between 1<sup>st</sup> and 2<sup>nd</sup> shell ligands in Zn-biomimetic complexes**

Gilles Frison\*, Gilles Ohanessian

Laboratoire des Mécanismes Réactionnels,  
Département de Chimie, Ecole Polytechnique, CNRS,

91128 Palaiseau Cedex, France.

Fax: + 00 33 (0)1 69 33 30 41

[gilles.frison@polytechnique.org](mailto:gilles.frison@polytechnique.org)

**Abstract:** Although theoretical methods are now available which give very accurate results, often comparable to the experimental ones, modeling chemical or biological interesting systems often requires, mainly due to computer limitations, less demanding and less accurate theoretical methods. Therefore, it is crucial to know the precision of such less reliable methods for relevant models and data. This has been done in this work for small zinc-active site models including O- ( $\text{H}_2\text{O}$  and  $\text{OH}^-$ ) and N-donor ( $\text{NH}_3$  and imidazole) ligands. Calculations using a number of quantum mechanical methods were carried out to determine their precision for geometries, coordination number relative stability, metal-ligand bond strengths, proton affinities and interaction energies between first and second shell ligands. We have found that obtaining chemical accuracy can be as straightforward as HF geometry optimization with a double- $\zeta$  plus polarization basis followed by a B3LYP energy calculation with a triple- $\zeta$  quality basis set including diffuse and polarization functions. The use of levels as low as PM3 geometry optimization followed by a B3LYP single-point energy calculation with a double- $\zeta$  quality basis including polarization functions already yields useful trends in bond length, proton affinities or bond dissociation energies, provided that appropriate caution is taken with the optimized structures. The reliability of these levels of calculation has been successfully demonstrated for real biomimetic cases.

**Key words:** QM calculations; Density-functional theory; Semi-empirical calculations; Carbonic Anhydrases; Biomimetic zinc complexes

## I-Introduction

Due largely to the importance of metals in biological systems, there has been growing interest toward modeling metal-binding sites in proteins.<sup>1</sup> Even though the past years have seen development of powerful methods based on density functional theory (DFT) and on resolution of identity approximations,<sup>2,3</sup> together with significant progress on computer capacity, the application of high-level quantum calculations to realistic chemical and/or biological systems still exceeds the present capacity of most research groups. Recent studies have thus been performed on model compounds with *ab initio* and DFT studies or on real systems with hybrid QM/MM methods where only part of the system is included in the quantum calculation.<sup>4-11</sup> In both cases, quantitative data are obtained only for models which negate the direct comparison of theoretical results with experimental ones and thus prevent evaluation of the accuracy of the computational methods. That raises the problem of the numerical uncertainty of results, especially when very small errors can induce a completely different chemical and biological behaviour. The aim of this paper is to provide a detailed calibration of several methods that are commonly used for either pure quantum mechanical or the QM core of hybrid QM/MM modeling. Both structural and energetic criteria are used, in order to assess method performance in a purpose-oriented way.

Many studies have been published testing the performance of various methodologies in the determination, among others, of the structures and energetics of transition-metal compounds.<sup>12-14</sup> They show that gradient-corrected DFT methods are in most cases superior to *ab initio* methods at the HF and MP2 levels for the calculations of transition-metal compounds. Indeed DFT performances are similar to or even better than the MP2 data, while the computational costs are less. DFT methods are however inferior to high-level *ab initio* methods such as CCSD(T) for very precise energy calculations.<sup>15,16</sup>

Zinc, which is, after iron, the second-most abundant transition metal in biology, is an important cofactor in all classes of enzymes. The importance of this element in all forms of life<sup>17-19</sup> has induced a particular interest in chemical biomimetic compounds involving zinc cation<sup>20-22</sup> and an increasing number of investigations of biologically-related zinc compounds based on quantum chemical methods.<sup>23-42</sup> As a  $d^{10}$  metal ion,  $Zn^{2+}$  is a “border-line” transition metal. Besides its chemical consequence, the fully occupied d-

shell leads to much simpler electronic structures and therefore also calculational requirements. Hence, semiempirical methods such as PM3, AM1 and MNDO/d have been shown to give satisfactory results for the calculation of zinc complexes, even if some large errors are observed.<sup>43</sup> Furthermore, unlike the other compounds including real transition metals, Zn<sup>2+</sup>-complexes have been studied at the *ab initio* level of calculation with accurate results.<sup>39,41,44-48</sup> More precisely, these studies show that geometry optimization at the HF level followed by a single point energy calculation at the MP2 level gives reasonable structures and relative energies. Other authors are more skeptical of the accuracy of HF geometry optimization compared to the DFT or MP2 methods.<sup>36,42,49-51</sup> The relative accuracy of DFT (mostly B3LYP functional) and MP2 level of calculations are also discussed by some authors with sometimes opposite conclusions. DFT is often comparable to MP2 for geometry optimization of mono-<sup>41,52</sup> and bi-nuclear<sup>47</sup> zinc enzyme sites or calculating proton dissociation energies<sup>53</sup> or proton transfer potential energy profiles.<sup>54</sup> However, DFT (six- *versus* four-coordination of hydrated Zn<sup>2+</sup> ions)<sup>49</sup> or MP2 (relative energies of proton dissociation energies)<sup>55</sup> could also be caught out. All these studies reveal the lack of a systematic evaluation of quantum chemical methods for biologically-related zinc compounds.

Furthermore, besides the fact that theoretical data are obtained mostly for model systems, experimental and theoretical data are often not directly comparable. This is especially the case for structural data for which comparison is made between an isolated molecule in the gas phase and a molecule which is part of a crystal and subject to crystal packing and intermolecular forces. The reliability of the evaluation of the computational method accuracy by comparison with available experimental data is thus questionable.

It is well known that chemical structure modification of an enzyme, even outside its active site, could largely modify its chemical reactivity. The protein engineering work of Christianson and Fierke on the indirect zinc ligands in carbonic anhydrase nicely illustrates this effect.<sup>56</sup> Recent theoretical studies on carbonic anhydrase also show that small models are inadequate to describe its mechanism which needed more extended models.<sup>26,28,57</sup> This relevance of extended models will contribute to the continuation of the use of more approximate methods.

The theoretical treatment of very small experimental effects requires very accurate computational methods. Conversely, the increasing size of the systems studied prohibits the use of such methods. It seems thus crucial to know in detail the precision of less accurate (but more applicable) theoretical methods compared to these very precise methods. This is the object of this study for the case of zinc complexes. Among the N (His), S (Cys) and O (Asp/Glu) amino acid side chain ligands found in zinc enzymes, only models of histidine side chain (NH<sub>3</sub> and imidazole) have been considered in this study. As in the active site, the zinc coordination sphere is completed by a water molecule which can be deprotonated. The scope of this study thus corresponds to models of [Zn<sup>2+</sup>(His)<sub>3</sub>(H<sub>2</sub>O)] core observed in a number of enzymes,<sup>58</sup> including carbonic anhydrase, and biomimetic complexes.<sup>22</sup> Our attention has been focussed on various data which have been shown to be of particular interest in studying catalytic metalloenzymes zinc-sites and related biomimetic compounds: geometrical structure,<sup>58,59</sup> zinc coordination number,<sup>60</sup> metal-water bond dissociation energy,<sup>21,61</sup> proton affinity of zinc-bound hydroxide<sup>21,61</sup> and first-second shell interaction energy.<sup>24,29,35,62,63</sup>

The first part of this study tackles evaluation of theoretical methods for zinc model complexes **1-11** (scheme 1). In order to avoid the bias discussed previously on the difference between experimental and theoretical data, computational references have been chosen. Comparison with these references gives an estimation of the absolute error made by using more approximate methods. On one hand, the smaller the absolute errors, the more accurate the corresponding method. On the other hand, the objective is to evaluate methods from a chemical point of view. This means that systematic absolute errors may be considered acceptable as long as relative errors are small (less than ~3% for bond lengths and less than ~5 kJ/mol for relative energies).

-----  
**Scheme 1**  
-----

In the second part of this study, trends obtained from the first part for small models have been applied to more extended, and thus more realistic, models **12-14** (Scheme 2). These

complexes are models of calix[6]arene-zinc biomimetic complexes synthesized by the group of Reinaud.<sup>64</sup> The X-Ray structure of the aqua-calixarene zinc complex shows a second water molecule located in the cavity formed by the phenyl groups.<sup>65</sup> This structure, modelled by compounds **12**, presents a hydrogen bond network around the zinc-bound water which is comparable to that of the active site of carbonic anhydrase II.<sup>66</sup>

-----

## Scheme 2

-----

## II-Methodology

Calculations were performed with the Gaussian 98 program suite.<sup>67</sup>

Four basis sets of growing flexibility were used, denoted as BS1, BS2, BS3 and BS4. BS1 consists of the 6-31G\* basis set for H, C, N and O and Wachters' [14s9p5d1f/9s5p3d1f] basis set for Zn.<sup>68</sup> BS2 consists of the 6-311+G\*\* basis set for H, C, N and O and the extended Wachters' [15s11p6d1f/10s7p4d1f] basis set for Zn. BS3 has been derived from BS2 by addition of different sets of polarization functions in which a second p for H, a second d for C, N and O (6-311+G(2d,2p) basis set) and a second f for Zn (Wachters' [15s11p6d2f/10s7p4d2f] basis set). BS4 consists of Dunning's aug-cc-pVTZ basis set for H, C, N and O and Wachters' [15s11p6d3f1g/10s7p4d3f1g] basis set for Zn.

Due to their large size, models **12-14** have been optimized with some simplification of the basis sets. Geometry optimizations have been conducted with BS1' and BS2', corresponding to BS1 and BS2 respectively, except for the C and H atoms of the 6 phenyl rings and of the 6 methylene groups linking the phenyl, for which the 6-31G basis set has been used. The same partition has been made for some single-point energy calculations with the BS3' basis set corresponding to BS3 except for the atoms of the 6 phenyl and methylene groups for which BS1 has been used.

Eight different methods, depending on the model considered, have been used for geometry optimization in combination with several of the above bases. The first is the PM3 semiempirical method<sup>69-71</sup> whose applicability has been previously explored.<sup>43,72</sup>

and which can be applied to large systems.<sup>73</sup> The second is Hartree-Fock (HF), which neglects electron correlation. The next two are post-Hartree-Fock methods which add electron correlation corrections to the HF method, either by perturbation (second-order Møller-Plesset (MP2) method) or by a coupled-cluster method (CCSD(T)). The last four are density functionals: we have used (i) the GGA functional BP86 which combines the exchange functional of Becke<sup>74</sup> and the correlation functional of Perdew (BP86),<sup>75</sup> (ii) the popular hybrid three-parameter functional developed by Becke, noted B3LYP, which includes Becke's gradient-corrected exchange functional<sup>76</sup> with the non-local correlation functional of Lee, Yang and Parr,<sup>77</sup> and the more recent hybrid one-parameter functionals noted (iii) mPW1PW91<sup>78</sup> and (iv) MPW1K.<sup>79</sup> The mPW1PW91 functional combines the Perdew/Wang 91 nonlocal correlation functional with the modified Perdew-Wang 91 one-parameter hybrid function to calculate the exchange energy.<sup>80</sup> The MPW1K functional is a modification of the mPW1PW91 functional. It should be noted, as already observed by other authors,<sup>81</sup> that optimization convergence criteria with the DFT methods are very difficult to attain. In this case, some of the minima could only be obtained when using the ultrafine integration grid, which renders DFT less efficient due to a significant increase of computation time.

All of the optimizations were done in the gas phase with no constraints. Harmonic vibrational frequencies were evaluated at the same level of theory to determine the nature (minima or transition states) of the stationary points.

Depending upon the case, single-point energy calculations of the optimized structures have been carried out at the B3LYP, MP2 and CCSD(T) levels in combination with BS1, BS2, BS3 and/or BS4. Basis set superposition error (BSSE) has been estimated for some cases at various levels.

In order to evaluate the accuracy of the various methods, we have compared them against *a priori* more reliable methods (called "reference methods") which have been used for each system (CCSD(T)/BS4//CCSD(T)/BS4 for **1**, **2** and **9**; CCSD(T)/BS3//MP2/BS2 for **3-6** and **10**; MP2/BS3//mPW1PW91/BS2 for **7**, **8** and **11**). The fact that geometric data obtained with CCSD(T)/BS4, MP2/BS2 and mPW1PW91/BS2 are almost identical for both **1** and **2** (see below) justifies this choice. For each complex, comparison has been

made between structural and energetic data obtained with the different methods and those obtained with the reference method (comparisons called “absolute”). We have also compared the variation of these data among the complexes (comparisons called “relative”).

### III-Results and Discussion

#### III.1-Theoretical methods evaluation on small models

The optimized structures for complexes **1-11** are shown in Figure 1. Before a quantitative description of the results is given, some general remarks should be made on the structures optimized at different levels. For H<sub>2</sub>O complexes **1**, **3**, **5A** and **7**, Zn is located in the H-O-H plane for all methods except BP86 and PM3 for which this planarity corresponds to a transition state for **1** or all complexes respectively. The corresponding minimum is obtained with an H<sub>2</sub>O bending of about 30°. Depending on the level of calculation, two different isomers have been obtained for **3** (denoted **3a** and **3b**) and **4** (denoted **4a** and **4b**). With PM3 and *ab initio* or DFT methods with BS1, geometry optimization yields isomer **4b** as a minimum and **4a** as a transition state, located between 1.0 and 7.0 kJ/mol above the minimum, whereas with BS2 **4a** is a minimum and **4b** is a transition state, located between 1.0 and 1.1 kJ/mol above the minimum. **3a** (one Zn-N bond eclipsed with an O-H bond) is obtained in all cases as a minimum except at the MP2/BS2 level for which **3a** is a transition state and **3b** (no Zn-N bond eclipsed by a O-H bond) is a minimum located 0.4 kJ/mol below **3a**. **5A** and **6** exhibit respectively one and two O··HN hydrogen bonds for all methods except PM3 for which respectively zero and one O··HN hydrogen bond are obtained. For complex **5B**, the three N and the Zn atoms form a plane and the two water molecules are almost symmetric relative to this plane, except with PM3 for which on water molecule is more tightly bound to the metal than the other. Only two of the three imidazole rings have been found to be parallel to the Zn-O bond in **8** except with PM3 for which the three rings have this orientation. Lastly, the Zn atom is located in the plane of the three nitrogen in **10** and **11** for all methods.

In every case, only results corresponding to minimum energy structures are presented here.

-----  
**Figure 1**  
-----

III.1.a-Absolute structural analysis

The main geometrical parameters obtained at various levels of theory for complexes **1-11** are displayed in Table 1.

-----  
**Table 1**  
-----

A first examination of Table 1 shows that, except for PM3, the different optimization methods give quite similar results for metal-ligand bond lengths and some more pronounced differences concerning long-range interaction lengths. A closer examination provides more details of these observations as outlined below.

*Metal-ligand bond lengths*

For **1** and **2** in which only one O ligand is bound to Zn, optimizations have been carried out up to CCSD(T)/BS4. Compared to this highest level of calculation, the closest results for **1** and **2** are obtained with CCSD(T)/BS3, MP2/BS2, mPW1PW91/BS2 and MPW1K/BS1. The largest differences with the CCSD(T)/BS4 optimized Zn-O bond lengths are obtained with PM3 (+0.083 Å in **1**), CCSD(T)/BS1 (+0.045 Å in **2**), HF/BS2 (+0.040 Å in **1**), BP86/BS1 (+0.039 Å in **2**), B3LYP/BS1 (+0.037 Å in **2**) and HF/BS1 (+0.032 Å in **1**). All other differences are smaller than 0.030 Å. Thus, except for PM3,<sup>43</sup> all Zn-O bond lengths are within 3 % of the reference values.

**10** and **11** possess only one kind of N ligand, respectively NH<sub>3</sub> and imidazole, bound to Zn. These optimizations have been carried out up to MP2/BS2 (for **10**) and mPW1PW91/BS2 (for **11**) which give accurate results compared to CCSD(T)/BS4 for **1** and **2**. In both cases, the various methods give comparable Zn-N bond lengths, the largest difference being obtained between HF/BS2 and MP2/BS1 for **10** (0.069 Å). The results

for the reference methods (2.009 Å for **10** and 1.958 Å for **11**) are in the average of the results panel. Thus all methods used for the optimization give Zn-N bond lengths within 3 % of the reference values.

Complexes **3-6** and **7-8** which possess both O and N ligands have been optimized with methods up to MP2/BS2 (for **3-6**) and mPW1PW91/BS2 (for **7-8**). The same observations as for **1-2** and **10-11** can be made. PM3 is the only method which fails to give accurate Zn-O bond lengths with the results always being between 0.05 and 0.17 Å too long. For the other methods, this error is smaller than 0.04 Å, except for complex **5B** which shows a large discrepancy (maximum deviation of 0.094 Å at the MPW1K/BS1 level). For the Zn-N bond lengths, all methods give results comparable to those obtained with the reference methods. The maximum deviation for Zn-N (0.074 Å) is obtained for **4** at the BP86/BS1 level.

Among all of the methods used, HF/BS2 is the one which gives the poorest Zn-N bond lengths, with overestimation from the reference method between 0.05 and 0.07 Å. Also HF/BS1 and B3LYP/BS2 always show longer Zn-N bond lengths than the reference methods, but to a minor extent (between +0.02 and +0.06 Å), whereas differences are even smaller for other methods. Complex **4** is the one which gives larger differences for Zn-N bond lengths, especially with PM3 and all *ab initio* and DFT methods with the BS1 basis set. This is due to the structural differences between **4a** (minimum with BS2) and **4b** (minimum with BS1 and PM3).

Some general remarks can be made from these results. First, for *ab initio* and DFT methods, extension from BS1 to BS2 basis sets induces a small lengthening (+0.035 Å maximum) of the Zn-N and Zn-O bonds for all complexes but **2**. We note however that further extension of the basis set to BS3 or BS4 induces a small shortening of the Zn-O bonds in **1** and **2** with CCSD(T).<sup>82</sup> This shows that BS1 probably induces a larger compensation of errors than BS2, which may lead in some cases to better results compared to more extended basis sets. The comparison between methods shows that MP2 and mPW1PW91 give very similar results with both BS1 and BS2, the largest difference being 0.017 Å (Zn-N in **5B** with BS1). Compared to these methods, B3LYP gives slightly longer bond lengths for both BS1 and BS2. Thus B3LYP/BS1 gives closer results than MP2/BS1 (or mPW1PW91/BS1) compared to MP2/BS2 (or mPW1PW91/BS2), and

B3LYP/BS2 is not markedly better than B3LYP/BS1. BP86/BS1 performs as well (or even better) as B3LYP/BS1 for Zn-O bond lengths whereas MPW1K/BS1 gives too short Zn-O bond lengths. Zn-N bond lengths for these last two levels are comparable to those obtained with MP2/BS1 or mPW1PW91/BS1. HF is less regular than correlated methods. Indeed HF/BS1 yields Zn-N and, to a minor extent Zn-OH<sub>2</sub>, bonds which are longer than those with the correlated methods with BS1, whereas Zn-OH are equal or slightly shorter. Compared to the correlated methods with BS2, HF/BS1 therefore gives accurate Zn-OH<sub>2</sub> bond lengths but less accurate Zn-N and Zn-OH bond lengths. The use of HF/BS2 does not improve HF/BS1 results and is even worse, probably due to error compensation with HF/BS1, as the Zn-N and Zn-OH<sub>2</sub> bonds clearly become too long. Lastly, PM3 gives accurate Zn-N bond lengths but Zn-O bond lengths which are noticeably too long. To obtain accurate metal-ligand bond lengths at the best quality/time ratio, geometry optimization should thus be done at the mPW1PW91/BS2 level or, for larger systems, at the B3LYP/BS1 level. If complete geometry optimization with DFT is not possible<sup>81</sup> then HF/BS1 is the best alternative.

#### *Long-range interaction lengths*

**5A** and **6** possess NH $\cdots$ O and OH $\cdots$ O hydrogen bonds to the water molecule that is added to **3** and **4**, respectively. Water molecule interaction with several ligands of **5A** (except with PM3) and **6** induces, for structural reasons, formation of a species in which the three atoms of the hydrogen bonds cannot be exactly aligned (figure 1). In Table 1 the distances between the heavy atoms of the NH $\cdots$ O (O<sup>2</sup>-N<sup>1</sup>) and OH $\cdots$ O (O<sup>1</sup>-O<sup>2</sup>) hydrogen bonds are given. The distance between the metal cation and the outer water oxygen (O<sup>2</sup>-Zn) is also indicated, since an electrostatic interaction could take place between Zn<sup>2+</sup> and O. Furthermore, this distance between zinc and a non-metal bound molecule is of interest, in order to elucidate mechanistic schemes in which this “external” molecule will bind to zinc by substituting another ligand or to give a pentavalent Zn<sup>2+</sup>.

MP2/BS2, B3LYP/BS2 and mPW1PW91/BS2 levels give very close results with B3LYP/BS2 distances being very slightly longer and the mPW1PW91/BS2 values being very slightly shorter than MP2/BS2 distances. Compared to the correlated methods with BS2, HF/BS2 gives hydrogen bonds which are around 0.1 Å too long. Moving from BS2

to BS1 for all methods induces a huge shortening (up to 0.15 Å) of the O<sup>2</sup>-N<sup>1</sup> and O<sup>2</sup>-Zn distances. The distance variation between O<sup>1</sup> and O<sup>2</sup> is less pronounced and depends on the complex. For BS1, **5A** and **6** show respectively longer and shorter O<sup>1</sup>-O<sup>2</sup> distances compared to BS2 with *ab initio* and DFT methods. These variations indicate that with BS1, the balance between the two kinds of hydrogen bonds is displaced in favour of the NH<sup>+</sup>⋯O bond in all cases. Compared to the correlated methods with BS2, all the methods with BS1 give noticeable differences. The largest variations compared to MP2/BS2 are obtained for the O<sup>2</sup>-N<sup>1</sup> distance with B3LYP/BS1 (-0.142 Å), MPW1K/BS1 (-0.159 Å), mPW1PW91/BS1 (-0.160 Å) and BP86/BS1 (-0.173 Å). This shows that correlated methods, especially DFT, give results which are sensitive to the basis sets and that some data could be worse than those obtained with HF. This also illustrates again that, probably due to error compensation, geometry optimization with BS1 gives more reliable results than with BS2.

As previously indicated, PM3 fails, compared to the other methods, to give the adequate hydrogen bonds in **5A** and **6**. Indeed the distance between O<sup>2</sup> and N<sup>1</sup> in **5A** (4.314 Å) is not in the range expected for a hydrogen bond. Likewise, only one O<sup>2</sup>-N<sup>1</sup> distance in **6** is below 4 Å whereas other methods give two O<sup>2</sup>-N<sup>1</sup> distances in the range of a hydrogen bond. The net result is that PM3 gives clearly longer O<sup>2</sup>-Zn distance (between +0.4 and +0.5 Å) than other methods, even if the OH<sup>+</sup>⋯O interaction seems to be correctly described.

This absolute structural analysis, and thus the accuracy of each level of calculation, is summarized comparing the percent difference between bond lengths obtained with each method relative to those obtained with the reference methods (Table 2).

-----  
**Table 2**  
 -----

The values obtained for MP2/BS2 and, to a minor extent, mPW1PW91/BS2, which are both used as reference methods, are by definition small. B3LYP/BS2 also gives rather

accurate geometries with a highest deviation of 1.4 %. For Zn complexes optimized with large basis sets such as BS2, DFT and MP2 methods give comparable structural results, unlike HF which is less accurate. With a modest basis set like BS1, all *ab initio* and DFT methods give acceptable results, none of them being clearly more or less accurate than the others. Indeed, correlated methods yield slightly more accurate metal-ligand bond lengths than does HF but are slightly less accurate for long-range interactions. PM3 gives inaccurate bond lengths except for the Zn-N bond lengths.

From this study, it can be recommended that B3LYP/BS1 and, to a lesser extent, HF/BS1 be used, as methods for geometry optimization of large zinc complexes.

### III.1.b-Relative structural analysis

When comparing several compounds within a series, obtaining reliable trends may be considered sufficient even if absolute errors for each species are not negligible. As a results not only have the structures of each optimized compound (“absolute analysis”) been examined but the variation of the bond lengths between various complexes (“relative analysis”) has been as well. For each level of calculation the variations between complexes **1-11** of the metal-ligand Zn-O and Zn-N bond lengths and of the long-range interaction lengths are depicted in Figures 2-4.

It is satisfying that in all cases and for all methods, the same qualitative bond length variations are observed. When an electron donating ligand is added to zinc, the Lewis acidity of the metal ion decreases, and all other metal-ligand bonds are lengthened. The same qualitative effect occurs when H<sub>2</sub>O is replaced by OH<sup>-</sup>. A lengthening of the Zn-N bonds after complexation of a water molecule to a L<sub>n</sub>Zn<sup>2+</sup> fragment on zinc and a second lengthening of the Zn-N bonds, accompanied by a shortening of the Zn-O bonds after deprotonation of this water molecule or due to the coordination of a second water molecule to zinc, are indeed observed. The same parallel variation is observed when adding or changing nitrogen ligands or when adding a second-shell ligand.

-----  
**Figure 2**  
-----

-----  
**Figure 3**  
-----

-----  
**Figure 4**  
-----

A comparison of each OH<sub>2</sub>/OH<sup>-</sup> pair of compounds reveals that all methods qualitatively reproduce the relative bond lengths variation between these couples. Indeed, the lengthening of the Zn-O (respectively shortening of the Zn-N) bonds from Zn-OH to Zn-OH<sub>2</sub> complexes increase in the order **1-2** < **5A-6** < **3-4** < **7-8** (Figure 2) (respectively **5A-6** < **3-4** < **7-8** for Zn-N (Figure 3)) for all methods.

These last trends illustrate the influence of the selected model (imidazole *vs* NH<sub>3</sub> metal ligands, inclusion of neighbouring water molecule) on the chemical results in terms of geometry and reactivity. In the context of the study of the active site of zinc enzymes, these trends show that small chemical effects cannot be correctly reproduced by limited models using NH<sub>3</sub> instead of imidazole or including only the first coordination shell.

The quantitative variation of the bond lengths also gives quite satisfying results. The differences in bond length variation are indeed in most cases not very large, even though some exceptions may be noted (cases of Zn-O bond between **1** and **2** or between **3** and **5B** (Figure 2) or of Zn-N bond between **5A** and **6** (Figure 3)). The absence of a NH<sup>+</sup>⋯O hydrogen bond in **5A** with PM3 also results in a large difference compared to other methods for the O<sup>2</sup>-N<sup>1</sup> long-range interaction (Figure 4). It should however be noted that while PM3 fails to describe Zn-O bond lengths, it succeeds quite accurately in reproducing the variation of these bond lengths, except for **5B** for which the creation of a second Zn-O bond is not reproduced.

The above results show that when comparing geometries within a series, all *ab initio* and DFT methods give reliable trends and may thus be recommended. Even PM3 is sufficient

for this purpose except for cases with modification of the coordination number and for long-range interactions which are in some cases poorly reproduced.

### III.1.c-Energetic analysis

In the preceding analyses, differences between the geometrical structures obtained with the various methods have been described. In the following the energetic data obtained at these geometries with various levels of calculation are examined. First, for a given compound and a given level of energy calculation, the total energies of structures optimized at several levels are compared. Then, the relative energy of isomers, the protonation energy (PE) of the zinc-bound hydroxide, the metal-water bond dissociation energy, and the first-second shell interaction energy are examined. The results obtained with each geometry and each level of calculation (absolute results) and also the variation of these data along the compounds (relative results) are presented. The objective is to estimate the influence of the geometry optimization on the energetical data, and of the importance of the level of calculation for energetics.

-----  
**Table 3**  
-----

#### *Relative energy of compounds 1-11*

Following geometry optimization, a single-point energy calculation for each compound has been carried out at a higher level of calculation (CCSD(T)/BS4 for **1** and **2**; CCSD(T)/BS3 for **3-6** and **10**; MP2/BS3 for **7, 8** and **11**). This allows a comparison of the relative energy of each geometry obtained with the various optimizing methods and thus gives an indication of the position on the potential energy surface for each geometry compared to the reference methods (Table 3). The higher the relative energy, the less accurate the geometry.

The results summarized in Table 3 confirm most of the conclusions drawn from the absolute structural analysis. MP2/BS2 and DFT/BS2 provide reliable geometries in

contrast to PM3. Correlated methods give better geometries with BS2 than with BS1 in contrast to HF.

Contrary to the hybrid DFT (hDFT) functional with BS1, BP86/BS1 gives larger relative energies. This is unexpected from the data in Tables 1 and 2 in which BP86/BS1 shows the same accuracy than the hDFT functional. A closer examination of the optimised geometry shows that BP86/BS1 leads to slightly longer (at least 0.01 Å) O-H and N-H bond compared to others methods. It is postulated that higher relative energies are due to this difference.

The relative energies obtained from HF/BS1 geometries are almost equivalent to those obtained from hDFT/BS1 or MP2/BS1. Quite unexpectedly, HF/BS1 geometries of **4** and **6** give lower relative energies than hDFT/BS1 and MP2/BS1 geometries. It is postulated that this is due for **4** to the difference between **4a** (minimum with BS2) and **4b** (minimum with BS1). For **6** the cause is the poor description of the two O<sup>2</sup>-N<sup>1</sup> bond lengths at the DFT and MP2/BS1 levels. On the other hand, results for the other molecules indicate a better accuracy for the hDFT/BS1 and MP2/BS1 optimized geometries. This is especially the case for molecules with imidazole ligands.

-----  
**Table 4**  
-----

*Relative stability of compounds 5A versus 5B*

**5A** and **5B** are isomers which differ by the number of direct metal ligands. In **5A**, zinc has a coordination number of 4 (three NH<sub>3</sub> ligands and one H<sub>2</sub>O ligand) and possesses a second water molecule as second-shell ligand. In **5B**, this second water molecule is directly bound to zinc which thus presents a coordination number of 5. If catalytic zinc active sites in their resting state show a coordination number of 4, changes to 5 are involved in catalytic processes taking place directly at Zn<sup>2+</sup>.<sup>17</sup> The energy difference between **5A** and **5B** computed at various levels (Table 4) gives a comparison between all methods for the coordination number preference of a dicationic zinc surrounded by nitrogen and oxygen ligands.<sup>83</sup> In all cases, **5A** has a lower energy than **5B**, indicating a

preference for a coordination number of 4, even if the difference is small. This is consistent both with experimental structures of  $\text{Zn}(\text{His})_3^{2+}$  active site including only one water molecule as metal ligand even if other water molecules are located as indirect ligands, and with the observation that coordination number can easily change around zinc.

Quantitative comparison of the relative stability at the level of optimization shows a great dependence upon the method/basis set used. With HF/BS1, **5A** and **5B** are almost isoenergetic whereas PM3 overestimates the difference. In all cases, moving from BS1 to BS2 increases the relative stability of **5A** compared to **5B** by about 10 kJ/mol. It is assumed that this is a consequence of the better description of the long range interaction in **5A**. It should however be noted that for a given level used for single point energy calculation, the energy difference between **5A** and **5B** is almost independent of the optimisation level. Single point energy calculations at the CCSD(T)/BS2, MP2/BS2 and MP2/BS3 levels give an energy difference almost equal to the 18 kJ/mol value computed with CCSD(T)/BS3. On the contrary, B3LYP/BS2 and B3LYP/BS3 overestimate it by about 10 kJ/mol.

These results imply that computing energy differences of isomers of different coordination numbers for large systems could be accurately done at MP2/BS2//HF-or-DFT/BS1 levels.

#### *Protonation energy (PE) of zinc-bound hydroxide*

The PE of zinc-bound hydroxide in **2**, **4**, **6** and **8** has been computed at various levels of geometry optimisation (Table 5). It shows clearly that the PE is greatly dependent upon the method/basis set used. PM3, HF and, to a lower extent, BP86 fail to give reliable values. For each method, the more extended the basis set, the smaller the PE (a reduction of 30-50 kJ/mol occurs from BS1 to BS2). It is assumed that this is a consequence of the better description of the hydroxide. Except for **2** where some differences up to 53 kJ/mol arise, hDFT and post-HF methods yield quite similar PE with a given basis set.

Another issue is the PE dependence upon the geometry. Table 6 gives the PE of **2** computed at various levels for each geometry obtained previously. Results for **4**, **6** and **8** are given as supporting information.

-----  
**Table 5**  
-----

-----  
**Table 6**  
-----

The data in Table 6 confirm that for each method used, the more extended the basis set, the weaker the PE. As expected, PE values for each method appear to converge to an infinite basis set limit value by increasing the basis set. This convergence is almost achieved with BS3, as differences between BS1, BS2 and BS3 are noticeable, whereas a change from BS3 to BS4 does not really modify the results. However, this infinite basis set limit value depends upon the method, which is especially true for the PE of **2** (around 250 kJ/mol with B3LYP, 280 kJ/mol with MP2 and 290 kJ/mol with CCSD(T)). PE of complexes **4**, **6** and **8** show less marked differences between B3LYP and MP2 or CCSD(T).

It is very interesting to note that the PE value obtained at any given level of calculation is only slightly dependent upon the optimized geometry. Indeed, for all single-point energy calculation methods, almost all geometries of **2** give a PE value within 1 kJ/mol of the reference CCSD(T)/BS4 geometry values. Exceptions involve mostly PM3 and HF/BS2 for which PE is either below (−3 to −10 kJ/mol) or above (+2 to +6 kJ/mol) the reference value respectively. CCSD(T)/BS1 and BP86/BS1 in three cases and B3LYP/BS1 in one case have also PE values above or below (between 2 and 3 kJ/mol) the reference value.

The computed PE data for **4**, **6** and **8** confirm this result even though the differences are slightly larger. MP2/BS2, B3LYP/BS2 and mPW1PW91/BS2 optimized geometries lead to, for each single-point energy calculation method, the same PE values within a maximum difference of 2 kJ/mol. MP2/BS1, B3LYP/BS1, mPW1PW91/BS1 and MPW1K/BS1 optimized geometries do the same with a maximum difference of 4 kJ/mol,

whereas BP86/BS1 gives slightly higher values by up to 9 kJ/mol. Differences between BS2- and BS1-correlated method geometries are greater, with a maximum of 13 kJ/mol. HF/BS1 geometries give PE value intermediate between those with BS2- and those with BS1-correlated methods. This shows, as previously noted in some cases for geometry optimization, that optimization at the HF/BS1 level gives slightly better PE results than optimization at the DFT or MP2/BS1 levels. HF/BS2 shows better results for **4**, **6** and **8** than for **2**, whereas PM3 geometries always give underestimated PE (between -5 and -20 kJ/mol).

The above results indicate that the relative PE values do not greatly depend upon the geometry or the single-point energy calculation method. Differences between the computed PE of **2**, **4**, **6** and **8** are in all cases relatively similar, even with PM3 geometries (approximately 380 kJ/mol between **2** and **4**, 20 kJ/mol between **4** and **6**, and 110 kJ/mol between **6** and **8**).

All these results imply that computing absolute PE values for large systems could be accurately done at MP2-or-B3LYP/BS3//HF-or-hDFT/BS1 levels. Relative PE are easier to obtain and could be confidently estimated by B3LYP/BS1//PM3 computations.

#### *Metal-water bond dissociation energy*

Table 7 displays metal-water bond dissociation energies computed at the level of optimization for **1**, **3**, **5B** and **7**. In order to dissect the binding interaction, these energies are broken down into several components. Figure 5 details the abbreviations used for this purpose.

-----  
**Table 7**  
-----

-----  
**Figure 5**  
-----

The preparation energy  $E_{\text{prep}}$  is the energy required to distort the fragments to their structures in the complex.  $E_{\text{prep}}$  depends strongly upon the fragment.  $\text{H}_2\text{O}$  stay mostly in the same geometry and its deformation costs only a few kJ/mol. Planar Zn complexes **10** and **11** are pyramidalized by the addition of one water molecule on the metal, whereas the tetrahedral arrangement around Zn in **3** is modified to give a slightly distorted trigonal bipyramid complex **5B**. This costs around 20 kJ/mol in all cases. It can be noted that, as shown by the X-ray crystal structure of native and apo carbonic anhydrase II,<sup>66</sup> the lack of the zinc cation does not induce modification of the enzyme geometry. Indeed, the three histidine side chains keep their pyramidal arrangement with and without  $\text{Zn}^{2+}$ . This rigidity of the enzyme conformation dictates that a geometry variation from planar to pyramidal structure around zinc could not take place in enzyme active sites, as well as for some biomimetic complexes bearing a tripodal ligand.<sup>22</sup> The same kind of nitrogen ligand rigidity is observed in the case of penta- (or higher) coordination.<sup>22,84</sup> It follows that models **3**, **5B** and **7** certainly overestimate the preparation energy compared to the actual experimental systems. For enzymes or rigid biomimetic complexes, experimental metal-water bond dissociation energies should be better evaluated by  $E_{\text{int}}$  than by  $E_{\text{bond}}$ . We note that  $E_{\text{prep}}$  is mostly independent of the method used.

The interaction energy  $E_{\text{int}}$  measures the interaction between two parts ( $\text{H}_2\text{O}$  and  $\text{Zn}(\text{ligands})$ ) of the complex, each part being in its optimized geometry in the complex. The interaction energy differs from the metal-water bond dissociation energy  $E_{\text{bond}}$  by the preparation energy. As noted above, its value could be used to compare the bond strength for cases with various deformations of the fragments, for example a rigid active site with low  $E_{\text{prep}}$  vs flexible theoretical models with larger  $E_{\text{prep}}$ . For **1**,  $E_{\text{int}}$  strongly depends upon the method used. Based on CCSD(T) results, HF and DFT methods lead to significant under- and overestimations, respectively. Results appear to be more uniform for **3**, **5B** and **7** whereas PM3 results are not reliable. Unexpectedly,  $E_{\text{int}}$  has a stable value (401 kJ/mol) at the CCSD(T)/BS1 to BS3 levels whereas CCSD(T)/BS4 has a noticeably higher value (411 kJ/mol) (*vide infra*).

BSSE is, as expected, essentially dependent upon basis set size and also upon the method used. HF gives lower BSSE values with BS1 than DFT and post-HF methods. From BS1

to BS2, a decrease of BSSE at the HF or DFT levels is observed which thus gives BSSE values under 10 kJ/mol.<sup>85,86</sup> MP2 (not show in Table 7) and CCSD(T) must be used with BS3 or BS4 to give such low BSSE values.

Bond dissociation energy,  $E_{\text{bond}}$ , depends upon the method used as does the interaction energy. This leads to significantly scattered values for **1**, while there is more consistency for **3**, **5B** and **7**. DFT methods using BS2 may be sufficiently accurate for biologically relevant models.

-----  
**Table 8**  
-----

The bond dissociation energy of **1** has been computed at various levels of calculations for each geometry obtained previously (Table 8). Results for **3**, **5B** and **7** are given as supporting information. Even though scattered values are obtained for **1** depending upon the method used (Table 7), it is clear from Table 8 that  $E_{\text{bond}}$  of **1** is almost independent of the method used to optimize geometries. At each level of calculation, all *ab initio* and DFT geometries give the same  $E_{\text{bond}}$  with a maximum difference of 2 kJ/mol. PM3 geometries lead to  $E_{\text{bond}}$  values which are always slightly underestimated, by 3-9 kJ/mol. This could be due to the longer Zn-O bonds in the PM3 geometries compared to the other methods. The same trend is observed for **3**, **5B** and **7**.

MP2 and CCSD(T) give comparable bond dissociation energies of **1**, mostly independent of the basis set used. Values obtained with B3LYP decrease slightly with improvement of the basis set size and are sometimes higher (for **1**) and sometimes lower (for **3**, **5B** and **7**) compared to the post-HF values. The basis set dependence is accentuated for **3**, **5B** and **7** with B3LYP and also observed with post-HF methods.

As noted previously, both with MP2 and CCSD(T), BS4 gives  $E_{\text{bond}}$  (or  $E_{\text{int}}$ ) of **1** around 10 kJ/mol higher than the basis set limit value which could be anticipated from BS1, BS2 and BS3 values. Additional computations (not shown in Tables) indicate that the same trend is obtained for compound **3** and, to a smaller extent ( $\sim +6$  kJ/mol), with B3LYP. We postulate that the different nature of the basis sets (Pople's basis sets for BS1-3,

Dunning's basis set for BS4) is responsible for this small discrepancy. This is confirmed by additional B3LYP calculations of  $E_{\text{bond}}$  based on the HF/BS1 optimized geometry of **1**. Dunning's basis sets, aug-cc-pVDZ, aug-cc-pVTZ (BS4) and aug-cc-pVQZ, give respectively 433, 435 and 437 kJ/mol (compared to the 438, 432 and 429 kJ/mol values obtained with BS1, BS2 and BS3 respectively. Table 8).

The above results indicate that the relative bond dissociation energy values do not depend upon the geometry. On the other hand, relative bond dissociation energies seem to be slightly dependent upon the single-point energy calculation method since B3LYP shows some differences compared to MP2 and CCSD(T). Nevertheless, as noted above, DFT/BS2 single point energy calculation may be sufficiently accurate for biologically relevant models.

It should be noted that this comparison of  $E_{\text{bond}}$  calculations will not be modified by BSSE correction. Indeed, BSSE evaluations with several levels of single-point calculation at various optimized geometries give a BSSE difference smaller than 1 kJ/mol.

From this study it is recommended that, for the calculation of accurate absolute metal-water bond dissociation energies, at least MP2-or-CCSD(T)/BS2//DFT-or-HF/BS1 be used. B3LYP/BS2//DFT-or-HF/BS1 may also be used for more crude values. Relative metal-water bond dissociation energies may already be approached at the B3LYP/BS1//PM3 level.

#### *First-second shell interaction energy*

The interaction energy between complexes **3** and **4** and a water molecule located in the second coordination shell has been computed. The interaction energy has been decomposed as shown in Figure 5 at each computational level used for geometry optimization (Table 9). The complex-second shell water bond dissociation energy  $E_{\text{bond}}$  has been also evaluated by single-point energy calculations at various levels for all the preceding geometries (Table 10).

-----

**Table 9**

-----

-----

**Table 10**

-----

The preparation energy  $E_{\text{prep}}$  shows noticeable variation with the level of optimization. In contrast to the data of Table 7, PM3 shows in Table 9 very low preparation energy values compared to *ab initio* and DFT levels. This could be due to the difference in optimized structures of **5A** and **6** between PM3 and the other methods as reflected by the number of OH...N hydrogen bond in the complexes (*vide supra*). **5A** gives the same  $E_{\text{prep}}$  with all *ab initio* and DFT whereas **6** shows large differences according to the basis set employed. This is correlated with the two different isomers of **4**. Indeed, going to **6** from **4a** is more favourable than from **4b**.

The interaction energy  $E_{\text{int}}$  is strongly underestimated at the PM3 level (see Table 7). For *ab initio* or DFT level,  $E_{\text{int}}$  is higher with BS1 than with BS2. This correlates with the hydrogen bond lengths which are generally larger with BS2 than with BS1.

As shown in Table 7, BSSE depends upon the method and the basis set used. BS1 always gives a high BSSE. With BS2, BSSE is low with the HF and DFT methods whereas it remains relatively high at the MP2 level.

The above results indicate that the  $E_{\text{bond}}$  or  $E_{\text{bond}}^{\text{c}}$  comparison is not obvious when optimized and calculated with a different method/basis set as it is influenced by many factors. It can be noted however that for each basis set, DFT and MP2 methods give comparable data.

Table 10 displays the bond dissociation energy of **5A** computed at various levels of calculation for each geometry obtained previously. Results for **6** are given as supporting information. Complex-second shell water bond dissociation energy  $E_{\text{bond}}$  of **5A** and **6** obtained at various levels of calculation do not depend on the optimized geometry, except for PM3 geometries which give a smaller dissociation energy by about 10 kJ/mol.  $E_{\text{bond}}$

depends mostly on the basis set used, with an energy decrease correlated with basis set improvement. Furthermore,  $E_{\text{bond}}$  seems to converge to a limit value with the basis set size increase. This is consistent with the metal-water bond dissociation energy variation if BS4 is excluded from the comparison (*vide supra*).  $E_{\text{bond}}$  changes only slightly with the method used. Indeed, B3LYP, MP2 and CCSD(T) yield comparable results (differences do not exceed 11 kJ/mol) in contrast to what was found for the metal-water bond energy. The relative bond dissociation energy values, in this case only evaluated by the difference between **5A** and **6**, do not depend on the geometry or on the single-point energy calculation method. Even PM3 geometries give almost the same differences compared to other methods. On the other hand, the relative bond dissociation energy seems to be slightly dependent on the single-point energy calculation basis set since BS1 shows lower values compared to BS2 or BS3 (~10 vs ~20 kJ/mol difference between  $E_{\text{bond}}$  of **5A** and **6**) with both B3LYP and post-HF methods.

These results show that  $E_{\text{bond}}$  is higher for **5A** than for **6**. This is unexpected from a chemical point of view as a hydrogen bond from a water molecule to a hydroxide ion is stronger than a hydrogen bond from a water molecule to another neutral water molecule. This is also not consistent with the geometries since **5A** has a longer hydrogen bond than **6**. It is postulated that the charge of the metal dication ( $\text{Zn}^{2+}$ ), and thus of the complex (+2 for **3** and **5A** and +1 for **4** and **6**) is responsible for this trend. This could be seen in two ways. On one hand, the higher charge of **3** compared to **4** may induce a higher electrostatic interaction with an outer water molecule. On the other hand, this charge effect may be indirect, with the  $\text{Zn}^{2+}\text{-OH}_2$  moiety being clearly more acidic than a free  $\text{OH}_2$  whereas the  $\text{Zn}^{2+}\text{-OH}$  moiety is less basic than a free  $\text{OH}$ .

It is recommended that first-second shell interaction energies be computed at least at the B3LYP-or-MP2/BS2//DFT-or-HF/BS1 level. B3LYP/BS1//PM3 level is mostly sufficient to give trends for first-second shell interaction energies within a series of similar complexes.

### III.2-Application to extended models

In this section, the relevance of some of the previous conclusions is tested by considering more complex models of zinc active sites based on a biomimetic complex synthesized and characterized by Reinaud's group.<sup>64,65</sup>

This model involves a tripodal ligand, in which three imidazoles again model the side chains of His94, His96 and His119 bound to Zn, but they are now tied together, via the ether linkages of a calix[6]arene ring. This structure accommodates several H-bonded water molecules, one of which is bound to Zn. Thus, the local zinc environment is structurally similar to the active site of carbonic anhydrase, with a relatively open side modeling the bottom of the enzyme binding pocket.

**13** and **14** have H<sub>2</sub>O and OH<sup>-</sup> bound to Zn, respectively, similarly to the **7/8** couple described above. **12** has a second water molecule H-bonded to the first, much as in **5A**, and corresponds to the X-ray characterized experimental structure.<sup>65</sup>

This model provides a means to test the accuracy of geometries obtained at relatively modest levels, by comparison with X-ray data. It also offers a significant size extension on which to test the previous conclusion that accurate energetics may be obtained without accurate geometries, and the reliability of energetic trends obtained at semi-empirical PM3 geometrics.

Geometry optimization of complexes **12-14** has been carried out at the PM3, HF/BS1', B3LYP/BS1' and mPW1PW91/BS2' levels. Figure 6 shows the optimized structure of **12** at the B3LYP/BS1' level. At all levels of optimization, as in the X-ray structure,<sup>65</sup> there are three hydrogen bonds, one between the two water molecules, and the other two between each water molecule and an oxygen of the calixarene arms. All calculations also reproduce the presence of an OH/ $\pi$  interaction between one phenyl ring and a hydrogen atom of the second water molecule. **13** shows two hydrogen bonds between the zinc-bound water molecule and two oxygen atoms of the calixarene ether linkages. Several structures have been found at some of the levels of optimization for **14**. They differ mostly by the existence or lack thereof hydrogen bonds between the zinc-bound hydroxide and an oxygen of the calixarene arms. The lowest energy structure, which correspond to the absence of a hydrogen bond, has been selected in all cases.

-----  
**Figure 6**  
-----

Table 11 displays the main geometrical parameters obtained at various levels of theory for complexes **12-14**.

-----  
**Table 11**  
-----

These results confirm the first part of this study. Metal-ligand bond lengths are rather similar at the HF or DFT levels with however Zn-N bonds that are slightly too long at the HF/BS1 level. PM3 gives Zn-O bonds that are clearly too long. Long range interaction lengths show, as previously, more differences between HF and DFT.

Comparison with the X-ray structure does not yield a clear-cut preference for a single method among HF/BS1', B3LYP/BS1' and mPW1PW91/BS2' as each of them reproduces some bond lengths well but some others less accurately.

Table 12 provides a comparison of the metal-ligand Zn-O and hydrogen bond ZnOH<sub>2</sub>...OH<sub>2</sub> bond length variations between complexes of this study. As observed in the first part of this study, all methods give the same amount of variation of a given bond length by modification of its environment, even if the bond length is only fairly described. Indeed, even if PM3 gives Zn-OH<sub>2</sub> and Zn-OH bonds that are too long (Tables 1 and 11), the increase of the Zn-O bond length from Zn-OH to Zn-OH<sub>2</sub> in a given complex is approximately correctly reproduced (entries 1-2 of Table 12). Furthermore, PM3 also gives the correct trends between these complexes. The increase of the Zn-O bond length for **7-8** is larger than for **13-14**.

-----  
**Table 12**  
-----

-----

The capability of PM3 to reproduce bond length variation is however less trustworthy in some cases (entries 3-4 of Table 12). Indeed, optimizations at the HF-or-DFT/BS1' level show that **13** and to a less extent **14** have shorter Zn-O bonds than **7** and **8**, respectively. These variations may be attributed to long-range effects of the calixarene (hydrogen bonding through the oxygen of the calixarene ether linkages,  $\pi$  interaction with the phenyl rings). PM3 gives the opposite trends which confirms its sometimes poor description of the long-range interactions.

Single point energy calculations have been performed for each geometry at the B3LYP/BS2 and B3LYP/BS3' for **12-14**. Table 13 gives the relative energy, protonation energy and complex-second shell water bond dissociation energy  $E_{\text{bond}}$  obtained at various levels of calculation for **12-14**.

-----  
**Table 13**  
-----

Relative energies at higher levels confirm, besides the best quality of mPW1PW91/BS2' level, that B3LYP/BS1 optimizations yield slightly more accurate geometries than those from HF/BS1, and that PM3 geometries are not reliable.

On the other hand, the protonation energy of **14** is almost independent of the geometry optimization level. Thus, **14** shows a clear and comparable increase in protonation energy relative to that of **8** for each of PM3 (ca. +130 kJ/mol), HF/BS1 (ca. +155 kJ/mol) and B3LYP/BS1 (ca. +145 kJ/mol) geometries. This difference in computed acidity of the zinc-bound water in **7** and **13** is in good agreement with the experimental finding that no water deprotonation occurs for the calix[6]arene-Zinc biomimetic complexes<sup>64,65</sup> compared to other model systems for which only the zinc-hydroxy form is stable.<sup>22</sup>

The same observation can be made for complex-second shell water bond dissociation energy. Indeed all calculations indicate that the second water molecule in the zinc-aqua

complex **12** is only weakly bound (by ca. 60-65 kJ/mol). This is in good agreement with experiment where this second water molecule was found to undergo fast exchange with free water on the NMR time scale at 298 K.<sup>65</sup>

#### **IV-Conclusion**

Although much progress has been made recently in theories, algorithms and computer capacity, the quest for larger and more realistic models remains a challenge for quantum chemistry. Even though the study of small models at a very high level of calculation can now be carried out, this is not the case for most chemical or biological systems which must be studied with faster, and thus less accurate, methods. In this work, small zinc-active site models including O- and N-donor ligands have been studied at low to very high levels of calculation, in order to evaluate the level of accuracy of the former methods. Furthermore some of these methods have been applied to larger zinc-active site models.

Optimization of geometry with the MP2 or the hybrid DFT functional B3LYP and mPW1PW91 methods with basis sets of triple- $\zeta$  quality with polarisation functions on all atoms and diffuse functions on heavy atoms (BS2) gives accurate results. However, at present, basis sets of this size remain largely unusable, even at the DFT level, to study large compounds of several tens of atoms. The use of less extended basis sets such as BS1 at the HF or the DFT levels results in only small differences compared to more accurate calculation levels. Even though HF/BS1 is slightly less accurate on average for geometries than B3LYP/BS1 or mPW1PW91/BS1, optimized structures are clearly more easily (and thus more quickly) obtained with HF/BS1 due to the convergence difficulty with DFT. In contrast to what is clearly established for transition metal compounds, HF/BS1 thus seems to be of a high quality/cost ratio for systems studied here including zinc. PM3 does not yield accurate geometries. However, it permits, as do all the other methods, the study of the geometry variation within a series of similar compounds, even though in some cases, especially when long-range interaction are present, some large discrepancies are found.

Accurate proton affinities or bond dissociation energies require MP2, CCSD(T) or possibly B3LYP single-point calculations with at least BS3 or possibly BS2. All

optimized geometries except those using PM3, and in some case BP86, can be used for this purpose. B3LYP or MP2 with smaller basis sets such as BS1 or BS2 may be successfully used, even with PM3 geometries, if the objective is to compare proton affinities or bond dissociation energies within a series of similar compounds. Conversely, this means that obtaining good energetic data by modeling does not necessarily imply that the geometrical data are accurate. Energetics cannot be computed reliably with PM3 or HF.

The quantum modeling of systems of biological interest, similar to systems studied here, with a chemical accuracy could be confidently obtained with the B3LYP/BS2//HF/BS1 level of calculation or higher. The use of lower levels such as B3LYP/BS1//PM3 could be recommended with some caution to study trends in bond length variations, proton affinities or bond dissociation energies.

### **Acknowledgments**

This work was supported by a grant of computer time at the Institut du Développement et des Ressources en Informatique Scientifique (IDRIS, project 0543) and at the Centre Informatique National de l'Enseignement Supérieur (CINES, project dcm2335). Financial support by the Centre National de la Recherche Scientifique (CNRS) and by Ecole Polytechnique (Palaiseau, France) is gratefully acknowledged.

### **Supporting Information Available:**

Proton affinity of the zinc-bound hydroxides of **4**, **6** and **8** obtained at various levels of calculation. Metal-water bond dissociation energy  $E_{\text{bond}}$  of **3**, **5B** and **7** obtained at various levels of calculation. Complex-second shell water bond dissociation energy  $E_{\text{bond}}$  of **6** obtained at various levels of calculation.

## References

1. Lovell, T.; Himo, F.; Han, W.-G.; Noodleman, L. *Coord Chem Rev* 2003, 238-239, 211-232.
2. Deglmann, P.; Furche, F.; Ahlrichs, R. *Chemical Physics Letters* 2002, 362, 511-518.
3. Sierka, M.; Hogekamp, A.; Ahlrichs, R. *J Chem Phys* 2003, 118, 9136-9148.
4. Siegbahn, P. E. M.; Blomberg, M. R. A. *Annu Rev Phys Chem* 1999, 50, 221-249.
5. Siegbahn, P. E. M.; Blomberg, M. R. A. *Chem Rev* 2000, 100, 421-437.
6. Gogonea, V.; Suarez, D.; van der Vaart, A.; Merz, K. M., Jr. *Curr Opin Struct Biol* 2001, 11, 217-223.
7. Ryde, U. *Curr Opin Struct Biol* 2003, 7, 136-142.
8. Siegbahn, P. E. M. *Quart Rev Biophys* 2003, 36, 91-145.
9. Shaik, S.; Kumar, D.; de Visser, S. P.; Altun, A.; Thiel, W. *Chem Rev* 2005, 105, 3188-3209.
10. Bruice, T. C. *Chem Rev* 2006, 106, 3119-3139.
11. Gao, J.; Ma, S.; Major, D. T.; Nam, K.; Pu, J.; Truhlar, D. G. *Chem Rev* 2006, 106, 3188-3209.
12. Frenking, G.; Antes, I.; Böhme, M.; Dapprich, S.; Ehlers, A. W.; Jonas, V.; Neuhaus, A.; Otto, M.; Stegmann, R.; Veldkamp, A.; Vyboishchikov, S. F. In *Reviews in Computational Chemistry*; Lipkowitz, K. B.; Boyd, D. B., Eds.; VCH: New York, 1996, p 63-144.
13. Cundari, T. R.; Benson, B. T.; Lutz, M. L.; Sommerer, S. O. In *Reviews in Computational Chemistry*; Lipkowitz, K. B.; Boyd, D. B., Eds.; VCH: New York, 1996, p 145-202.
14. Diedenhofen, M.; Wagener, T.; Frenking, G. In *Computational Organometallic Chemistry*; Cundari, T., Ed.; Marcel Dekker: New York, 2001, p 69-121.
15. Ghosh, A.; Taylor, P. R. *Curr Opin Chem Biol* 2003, 7, 113-124.
16. Dunning, T. H., Jr. *J Phys Chem A* 2000, 104, 9062-9080.
17. Lipscomb, W. N.; Strater, N. *Chem Rev* 1996, 96, 2375-2433.

18. Auld, D. S. In *Structure and Bonding: Metal Site in Proteins and Models*; Sadler, P. J., Ed.; Springer: Berlin, 1997, p 29-50.
19. Maret, W. *Biochemistry* 2004, 43, 3301-3309.
20. Kimura, E.; Koike, T.; Shionoya, M. In *Structure and Bonding: Metal Site in Proteins and Models*; Sadler, P. J., Ed.; Springer: Berlin, 1997, p 1-28.
21. Parkin, G. In *Probing of proteins by metal ions and their low-molecular-weight complexes*; Sigel, A.; Sigel, H., Eds.; M. Dekker, Inc.: New York, 2001, p 411-460.
22. Parkin, G. *Chem Rev* 2004, 104, 699-767.
23. Estiu, G.; Suarez, D.; Merz, K. M., Jr. *J Comput Chem* 2006, 27, 1240-1262.
24. Lin, Y.-L.; Lee, Y.-M.; Lim, C. *J Am Chem Soc* 2005, 127, 11336-11347.
25. Morlok, M. M.; Janak, K. E.; Zhu, G.; Quarless, D. A.; Parkin, G. *J Am Chem Soc* 2005, 127, 14039-14050.
26. Marino, T.; Russo, N.; Toscano, M. *J Am Chem Soc* 2005, 127, 4242-4253.
27. Linder, D. P.; Rodgers, K. R. *J Phys Chem B* 2004, 108, 13839-13849.
28. Bottoni, A.; Lanza, C. Z.; Miscione, G. P.; Spinelli, D. *J Am Chem Soc* 2004, 126, 1542-1550.
29. Lin, Y.; Lim, C. *J Am Chem Soc* 2004, 126, 2602-2612.
30. Schenk, S.; Kesselmeier, J.; Anders, E. *Chem Eur J* 2004, 10, 3091-3105.
31. Olsen, L.; Antony, J.; Ryde, U.; Adolph, H.-W.; Hemmingsen, L. *J Phys Chem B* 2003, 107, 2366-2375.
32. Bergquist, C.; Fillebeen, T.; Morlok, M. M.; Parkin, G. *J Am Chem Soc* 2003, 125, 6189-6199.
33. Rulisek, L.; Havlas, Z. *J Phys Chem B* 2003, 107, 2376-2385.
34. Cammi, R.; Lanfranchi, M.; Marchio, L.; Mora, C.; Paiola, C.; Pellinghelli, M. A. *Inorg Chem* 2003, 42, 1769-1778.
35. Dudev, T.; Lim, C. *Chem Rev* 2003, 103, 773-787.
36. Xia, J.; Shi, Y.-B.; Zhang, Y.; Miao, Q.; Tang, W.-X. *Inorg Chem* 2003, 42, 70-77.
37. Hasegawa, K.; Ono, T.-A.; Noguchi, T. *J Phys Chem A* 2002, 106, 3377-3390.
38. Simonson, T.; Calimet, N. *Proteins* 2002, 49, 37-48.

39. Bräuer, M.; Pérez-Lustres, J. L.; Weston, J.; Anders, E. *Inorg Chem* 2002, 41, 1454-1463.
40. Deerfield, D. W.; Carter, C. W.; Pedersen, L. G. *Int J Quantum Chem* 2001, 83, 150-165.
41. Diaz, N.; Suarez, D.; Merz, K. M., Jr. *J Am Chem Soc* 2000, 122, 4197-4208.
42. Ryde, U. *Biophys J* 1999, 77, 2777-2787.
43. Bräuer, M.; Kunert, M.; Dinjus, E.; Klussmann, M.; Doring, M.; Gorls, H.; Anders, E. *Theochem-J Mol Struct* 2000, 505, 289-301 and references cited therein.
44. Isaev, A.; Scheiner, S. *J Phys Chem B* 2001, 105, 6420-6426.
45. Bräuer, M.; Anders, E.; Sinnecker, S.; Koch, W.; Rombach, M.; Brombacher, H.; Vahrenkamp, H. *Chem Commun* 2000, 647-648.
46. Rogalewicz, F.; Hoppilliard, Y.; Ohanessian, G. *Int J Mas Spectrom* 2000, 201, 307-320.
47. Zhan, C.-G.; de Souza, O. N.; Rittenhouse, R.; Ornstein, R. L. *J Am Chem Soc* 1999, 121, 7279-7282.
48. Zheng, Y.-J.; Merz, K. M., Jr. *J Am Chem Soc* 1992, 114, 10498-10507.
49. Diaz, N.; Suarez, D.; Merz, K. M., Jr. *Chem Phys Lett* 2000, 326, 288-292.
50. Dudev, T.; Lim, C. *J Phys Chem B* 2001, 105, 10709-10714.
51. Rulisek, L.; Sponer, J. *J Phys Chem B* 2003, 107, 1913-1923.
52. Diaz, N.; Suarez, D.; Merz, K. M., Jr. *J Am Chem Soc* 2001, 123, 9867-9879.
53. El Yazal, J.; Roe, R. R.; Pang, Y. P. *J Phys Chem B* 2000, 104, 6662-6667.
54. Chen, H.; Li, S.; Jiang, Y. *J Phys Chem A* 2003, 107, 4652-4660.
55. El Yazal, J.; Pang, Y. P. *Theochem-J Mol Struct* 2001, 545, 271-274.
56. Christianson, D. W.; Fierke, C. A. *Acc Chem Res* 1996, 29, 331-339.
57. Loferer, M. J.; Tautermann, C. S.; Loeffler, H. H.; Liedl, K. R. *J Am Chem Soc* 2003, 125, 8921-8927.
58. Auld, D. S. *Biometals* 2001, 14, 271-313.
59. Christianson, D. W. *Adv Protein Chem* 1991, 42, 281-355.
60. Dudev, M.; Wang, J.; Dudev, T.; Lim, C. *J Phys Chem B* 2006, 110, 1889-1895.
61. McCall, K. A.; Huang, C. C.; Fierke, C. A. *J Nutr* 2000, 130, 1437S-1446S.

62. Dudev, T.; Lin, Y.-L.; Dudev, M.; Lim, C. *J Am Chem Soc* 2003, 125, 3168-3180.
63. Dudev, T.; Lim, C. *J Am Chem Soc* 2002, 124, 6759-6766.
64. Sénèque, O.; Rager, M.-N.; Giorgi, M.; Reinaud, O. *J Am Chem Soc* 2000, 122, 6183-6189.
65. Sénèque, O.; Rager, M. N.; Giorgi, M.; Reinaud, O. *J Am Chem Soc* 2001, 123, 8442-8443.
66. Hakansson, K.; Carlsson, M.; Svensson, L. A.; Liljas, A. *J Mol Biol* 1992, 227, 1192-1204.
67. Frisch, M. J.; Trucks, G. W.; Schlegel, H. B.; Scuseria, G. E.; Robb, M. A.; Cheeseman, J. R.; Zakrzewski, V. G.; Montgomery, J. A., Jr.; Stratmann, R. E.; Burant, J. C.; Dapprich, S.; Millam, J. M.; Daniels, A. D.; Kudin, K. N.; Strain, M. C.; Farkas, O.; Tomasi, J.; Barone, V.; Cossi, M.; Cammi, R.; Mennucci, B.; Pomelli, C.; Adamo, C.; Clifford, S.; Ochterski, J.; Petersson, G. A.; Ayala, P. Y.; Cui, Q.; Morokuma, K.; Malick, D. K.; Rabuck, A. D.; Raghavachari, K.; Foresman, J. B.; Cioslowski, J.; Ortiz, J. V.; Baboul, A. G.; Stefanov, B. B.; Liu, G.; Liashenko, A.; Piskorz, P.; Komaromi, I.; Gomperts, R.; Martin, R. L.; Fox, D. J.; Keith, T.; Al-Laham, M. A.; Peng, C. Y.; Nanayakkara, A.; Gonzalez, C.; Challacombe, M.; Gill, P. M. W.; Johnson, B.; Chen, W.; Wong, M. W.; Andres, J. L.; Gonzalez, C.; Head-Gordon, M.; Replogle, E. S.; Pople, J. A.; Gaussian, Inc.: Pittsburgh, PA, 1998.
68. Wachters, A. J. *J Chem Phys* 1970, 52, 1033-1036.
69. Stewart, J. J. P. *J Comput Chem* 1989, 10, 209-220.
70. Stewart, J. J. P. *J Comput Chem* 1989, 10, 221-264.
71. Stewart, J. J. P. *J Comput Chem* 1991, 12, 320-341.
72. Anh, N. T.; Frison, G.; Solladié-Cavallo, A.; Metzner, P. *Tetrahedron* 1998, 54, 12841-12852.
73. Stewart, J. J. P. *Theochem-J Mol Struct* 1997, 401, 195-205.
74. Becke, A. D. *Phys Rev A* 1988, 38, 3098-3100.
75. Perdew, J. P. *Phys Rev B* 1986, 33, 8822-8824.
76. Becke, A. D. *J Chem Phys* 1993, 98, 5648-5652.
77. Lee, C. T.; Yang, W. T.; Parr, R. G. *Phys Rev B* 1988, 37, 785-789.

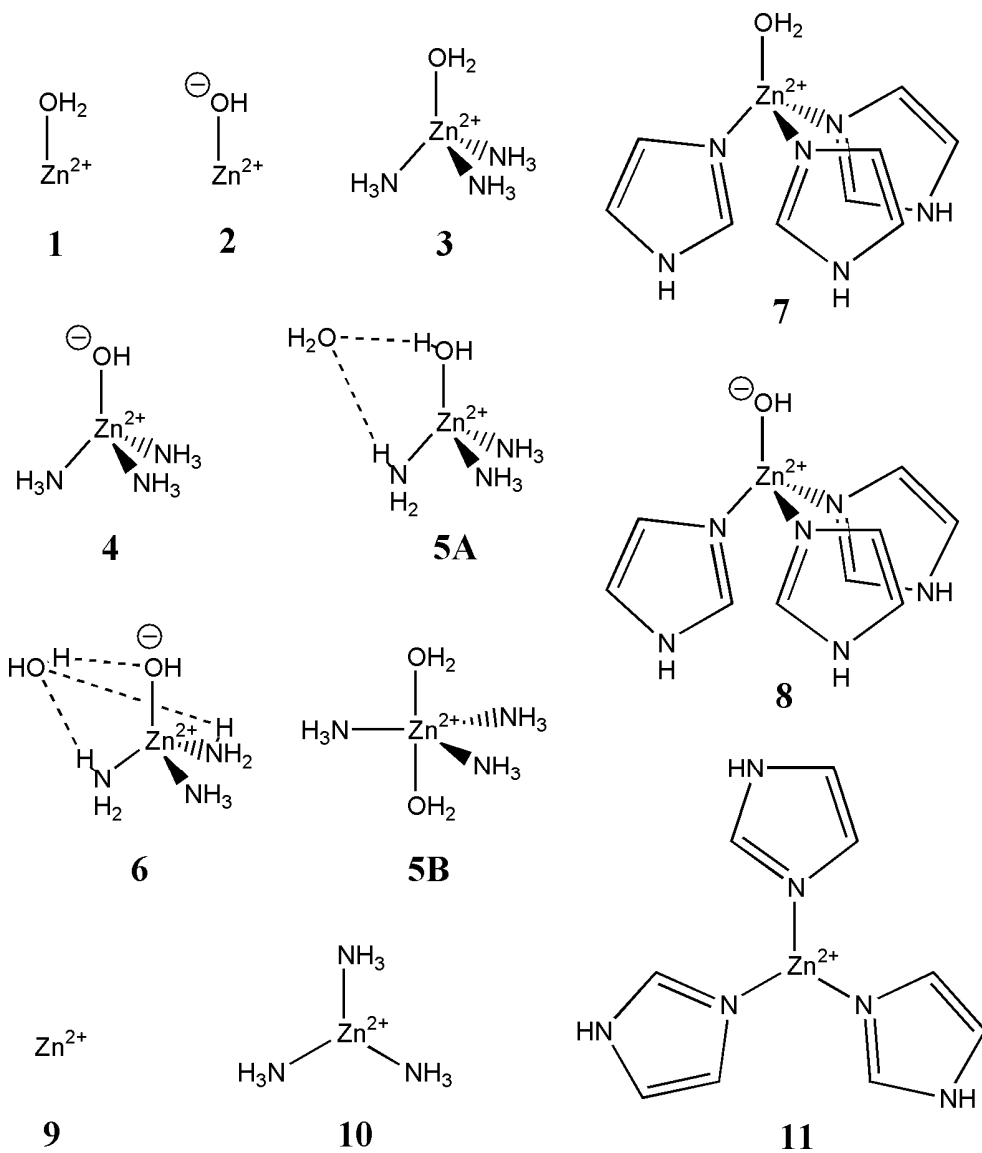
78. Adamo, C.; Barone, V. *J Chem Phys* 1998, 108, 664-675.
79. Lynch, B. J.; Fast, P. L.; Harris, M.; Truhlar, D. G. *J Phys Chem A* 2000, 104, 4811-4815.
80. Perdew, J. P.; Wang, Y. *Phys Rev B* 1992, 45, 13244-13249.
81. Peschke, M.; Blades, A. T.; Kebarle, P. *J Am Chem Soc* 2000, 122, 1492-1505.
82. The same effect is also observed with B3LYP for **1-4** (results not shown).
83. Fatmi, M. Q.; Hofer, T. S.; Randolph, B. R.; Rode, B. M. *J Phys Chem B* 2007, 111, 151-158.
84. Hakansson, K.; Wehnert, A. *Journal of Molecular Biology* 1992, 228, 1212-1218.
85. Dudev, T.; Lim, C. *J Am Chem Soc* 2000, 122, 11146-11153.
86. Tiraboschi, G.; Gresh, N.; Giessner-Prettre, C.; Pedersen, L. G.; Deerfield, D. W. *J Comput Chem* 2000, 21, 1011-1039.

## **List of Schemes**

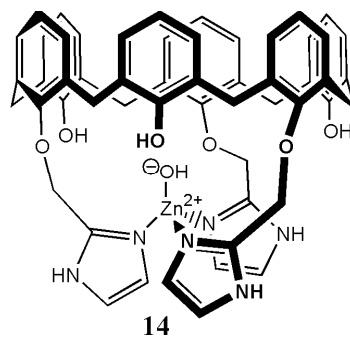
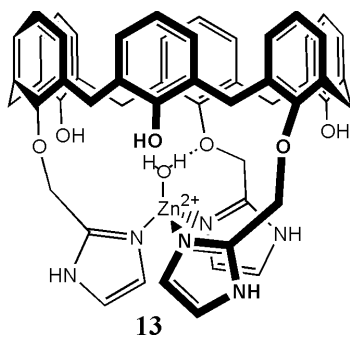
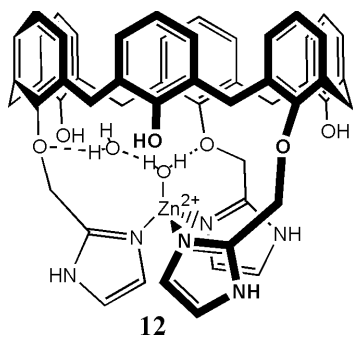
**Scheme 1.** small zinc model complexes.

**Scheme 2.** extended zinc model complexes.

Scheme 1



**Scheme 2**



## **List of Figures**

**Figure 1.** Geometrical structures of compounds **1-11**.

**Figure 2.** Relative Zn-O bond length variations

**Figure 3.** Relative Zn-N bond length variations

**Figure 4.** Relative long-range interaction length variations

**Figure 5.** Definition of abbreviations used to describe bond energies

**Figure 6.** Geometrical structures of compound **12**.

Figure 1

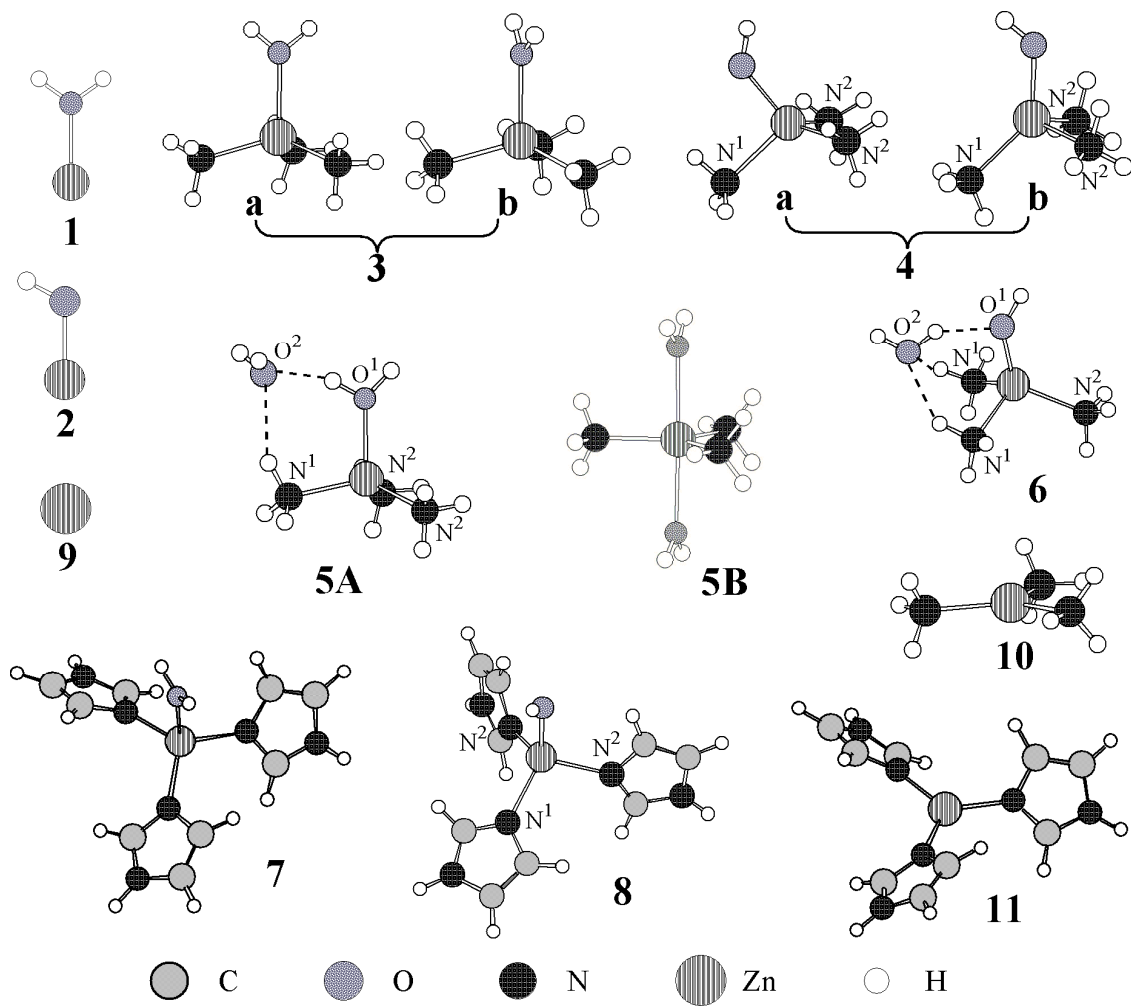


**Figure 2**

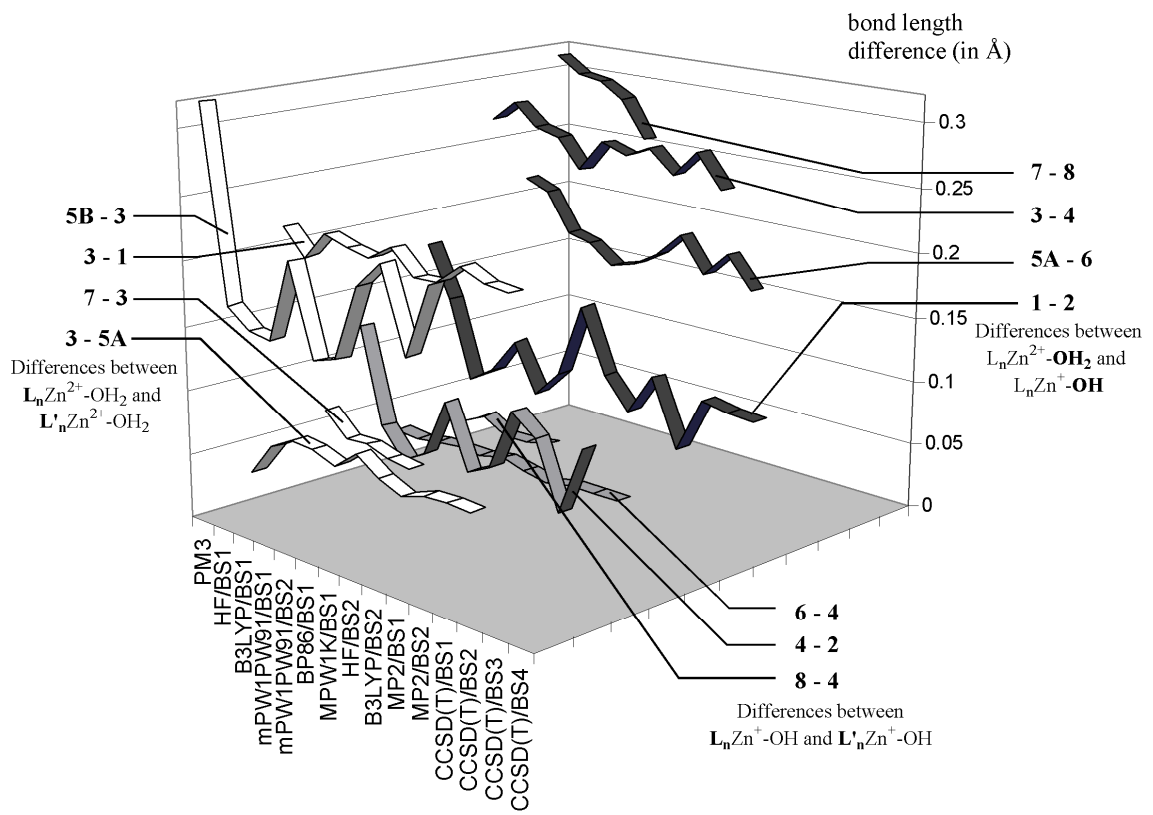


**Figure 3**

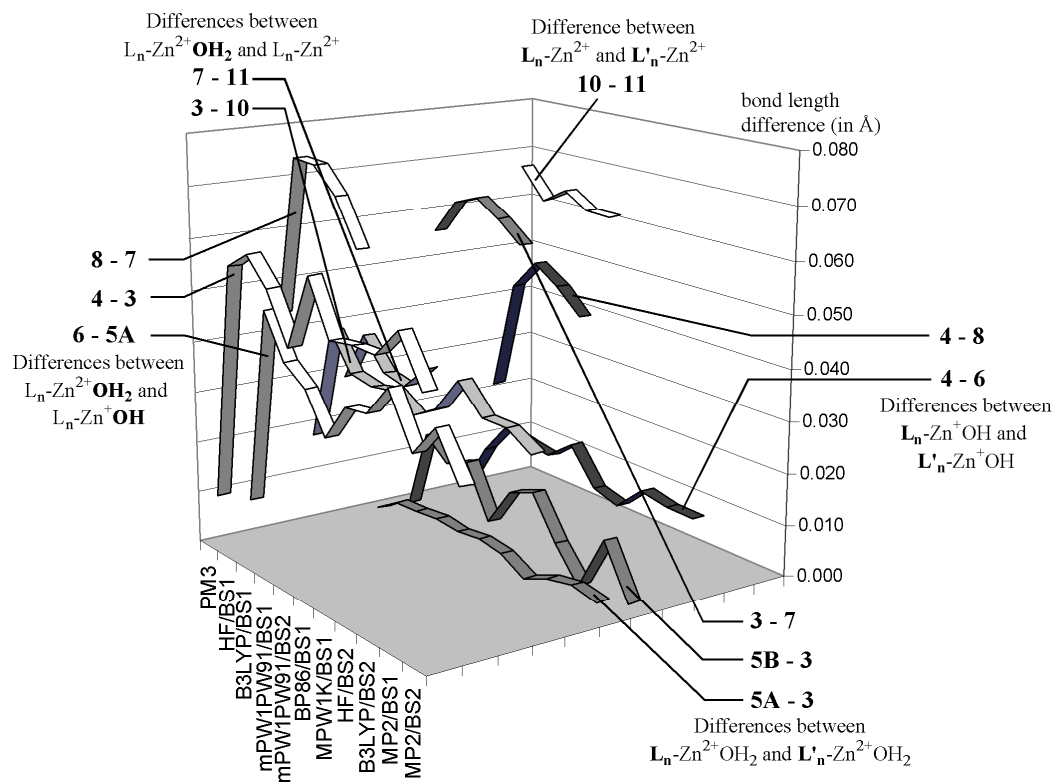
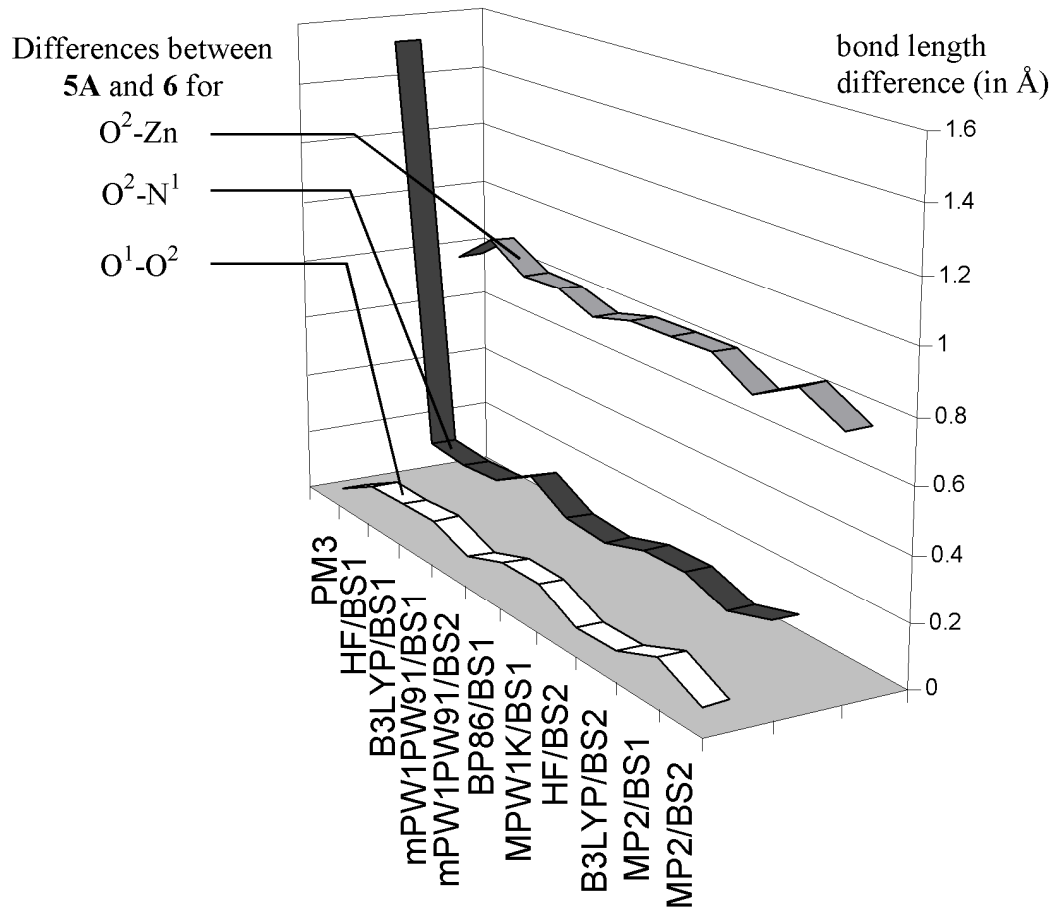


Figure 4



**Figure 5**

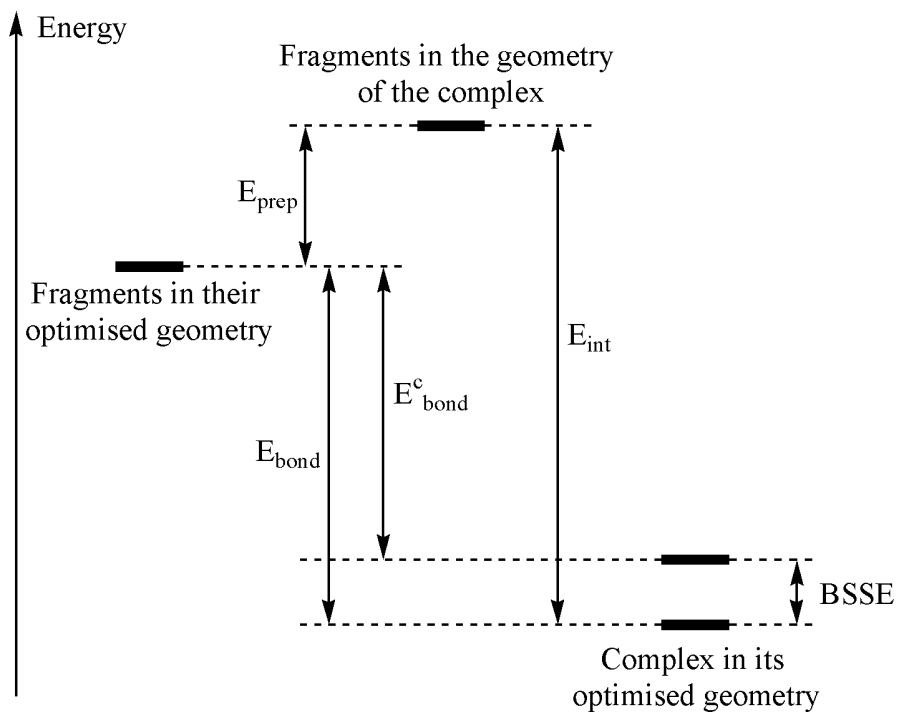
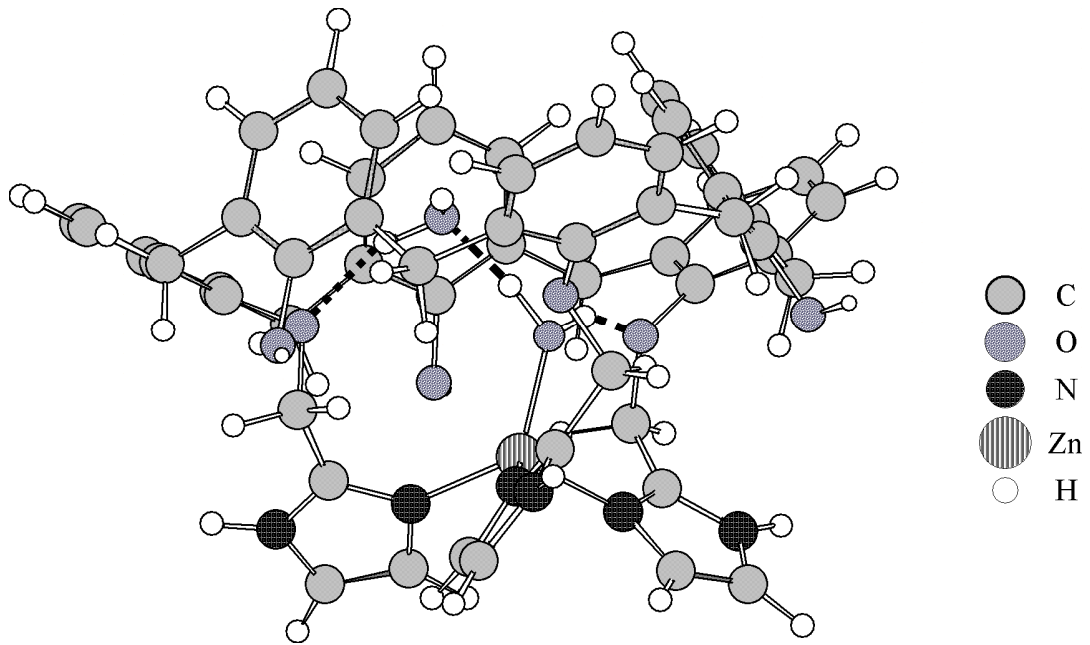


Figure 6



## List of Tables

**Table 1.** Comparison of bond lengths (in Å) calculated for **1-11** with various methods.

**Table 2.** Accuracy of each level of calculation for each type of bond in percent.

**Table 3.** Comparison of the relative energy (in kJ/mol) of **1-11** with various methods.

**Table 4.** Relative stability (in kJ/mol) of **5A** versus **5B** obtained at various levels of calculation.

**Table 5.** Protonation energy (in kJ/mol) of zinc-bound hydroxide obtained at the level of optimization.

**Table 6.** Protonation energy (in kJ/mol) of zinc-bound hydroxide of **2** obtained at various levels of calculation.

**Table 7.** Metal-water bond dissociation energy (in kJ/mol) computed at the level of geometry optimization.

**Table 8.** Metal-water bond dissociation energy  $E_{\text{bond}}$  (in kJ/mol) of **1** obtained at various levels of calculation.

**Table 9.** First-second shell interaction energy<sup>b</sup> (in kJ/mol) obtained at the level of geometry optimization.

**Table 10.** complex-second shell water bond dissociation energy  $E_{\text{bond}}$  of **5A** (in kJ/mol) obtained at various levels of calculation.

**Table 11.** Main geometrical parameters ( $d$ , in Å) obtained for complexes **12-14** and relative differences ( $\Delta$ ) from the experimental geometry with various methods.

**Table 12.** relative Zn-O and O···O bond lengths variation (in Å) obtained with various methods.

**Table 13.** Relative energy, protonation energy and first-second shell interaction energy (in kJ/mol) obtained at various levels of calculation for **12-14**.

**Table 1.** Comparison of bond lengths (in Å) calculated for **1-11** with various methods.

Method	PM3	HF		BP86	B3LYP		mPW1PW91		MPW1K	MP2		CCSD(T)			
		BS1	BS2		BS1	BS1	BS2	BS1		BS2	BS1	BS1	BS2	BS1	BS2
<b>1</b>															
Zn-O	1.945	1.894	1.902	1.875	1.870	1.882	1.863	1.874	1.859	1.863	1.874	1.870	1.883	1.871	1.862
<b>2</b>															
Zn-O	1.769	1.759	1.746	1.798	1.796	1.775	1.777	1.760	1.761	1.779	1.758	1.804	1.775	1.766	1.759
<b>3</b>															
Zn-O	2.160	2.089	2.104	2.094	2.087	2.100	2.074	2.081	2.060	2.073	2.082	b	b	b	b
Zn-N <sup>a</sup>	2.054	2.077	2.097	2.027	2.036	2.071	2.024	2.053	2.023	2.023	2.042	b	b	b	b
<b>4</b>															
Zn-O	1.891	1.804	1.835	1.828	1.818	1.849	1.810	1.840	1.801	1.801	1.835	b	b	b	b
Zn-N <sup>1</sup>	2.061	2.110	2.147	2.019	2.034	2.123	2.023	2.100	2.027	2.028	2.093	b	b	b	b
Zn-N <sup>2a</sup>	2.065	2.145	2.148	2.121	2.127	2.121	2.107	2.098	2.096	2.105	2.088	b	b	b	b
<b>5A</b>															
Zn-O <sup>1</sup>	2.133	2.036	2.054	2.023	2.023	2.043	2.011	2.025	2.002	2.015	2.025	b	b	b	b
Zn-N <sup>1</sup>	2.054	2.074	2.093	2.025	2.034	2.070	2.022	2.053	2.021	2.021	2.043	b	b	b	b
Zn-N <sup>2a</sup>	2.054	2.083	2.100	2.034	2.042	2.076	2.031	2.058	2.029	2.030	2.046	b	b	b	b
O <sup>1</sup> -O <sup>2</sup>	2.692	2.742	2.742	2.657	2.672	2.657	2.653	2.627	2.650	2.703	2.647	b	b	b	b
O <sup>2</sup> -N <sup>1</sup>	4.314	3.195	3.292	3.008	3.039	3.183	3.021	3.173	3.022	3.081	3.181	b	b	b	b
O <sup>2</sup> -Zn	4.303	3.854	3.900	3.752	3.764	3.822	3.744	3.798	3.737	3.793	3.804	b	b	b	b

<b>5B</b>															
Zn-O <sup>a</sup>	2.483 <sup>c</sup>	2.260	2.317	2.243	2.244	2.333	2.228	2.299	2.215	2.245	2.309	b	b	b	b
Zn-N <sup>a</sup>	2.052	2.093	2.103	2.039	2.048	2.071	2.038	2.057	2.037	2.034	2.043	b	b	b	b
<b>6</b>															
Zn-O <sup>1</sup>	1.919	1.830	1.860	1.861	1.847	1.877	1.840	1.869	1.829	1.829	1.863	b	b	b	b
Zn-N <sup>1a</sup>	2.064	2.118	2.134	2.076	2.085	2.109	2.068	2.086	2.062	2.067	2.077	b	b	b	b
Zn-N <sup>2</sup>	2.059	2.133	2.143	2.053	2.068	2.101	2.055	2.080	2.059	2.061	2.072	b	b	b	b
O <sup>1</sup> -O <sup>2</sup>	2.676	2.655	2.704	2.557	2.583	2.612	2.552	2.576	2.546	2.600	2.611	b	b	b	b
O <sup>2</sup> -N <sup>1a</sup>	2.779	2.994	3.052	2.802	2.850	2.938	2.820	2.897	2.825	2.881	2.937	b	b	b	b
O <sup>2</sup> -Zn	3.530	2.976	3.083	2.943	2.964	3.076	2.935	3.033	2.926	2.968	3.048	b	b	b	b
<b>7</b>															
Zn-O	2.221	2.132	b	b	2.131	b	2.112	2.116	b	b	b	b	b	b	b
Zn-N <sup>a</sup>	1.998	2.014	b	b	1.971	b	1.962	1.995	b	b	b	b	b	b	b
<b>8</b>															
Zn-O	1.909	1.832	b	b	1.835	b	1.827	1.861	b	b	b	b	b	b	b
Zn-N <sup>1</sup>	2.036	2.084	b	b	2.026	b	2.015	2.048	b	b	b	b	b	b	b
Zn-N <sup>2a</sup>	2.045	2.092	b	b	2.056	b	2.041	2.061	b	b	b	b	b	b	b
<b>10</b>															
Zn-N <sup>a</sup>	2.036	2.036	2.056	1.996	2.002	2.035	1.991	2.019	1.989	1.987	2.009	b	b	b	b
<b>11</b>															
Zn-N <sup>a</sup>	1.969	1.975	b	b	1.938	b	1.930	1.958	b	b	b	b	b	b	b

<sup>a</sup> mean value. <sup>b</sup> geometry optimisation not carried out at this level. <sup>c</sup> the two water molecules are distinct with respective 2.220 and 2.746 Å Zn-O bond lengths.

**Table 2.** Accuracy of each level of calculation for each type of bond in percent.

	Zn-OH <sub>2</sub>	Zn-OH	Zn-N	OH <sup>⋯</sup> N	OH <sup>⋯</sup> O	O <sup>⋯</sup> Zn	Mean value
PM3 <sup>a</sup>	5.2	2.3	0.7	20.5	2.1	14.5	7.6
HF/BS1 <sup>a</sup>	1.1	1.3	1.7	1.2	2.6	1.8	1.6
HF/BS2 <sup>b</sup>	1.2	0.3	2.7	3.7	3.6	1.8	2.2
BP86/BS1 <sup>b</sup>	1.1	0.7	1.0	5.0	1.2	2.4	1.9
B3LYP/BS1 <sup>a</sup>	0.9	1.3	0.8	3.7	1.0	1.9	1.6
B3LYP/BS2 <sup>b</sup>	1.0	0.8	1.4	0.0	0.2	0.7	0.7
mPW1PW91/BS1 <sup>a</sup>	1.0	1.4	1.2	4.5	1.2	2.6	2.0
mPW1PW91/BS2 <sup>a</sup>	0.2	0.2	0.3	0.8	1.0	0.3	0.5
MPW1K/BS1 <sup>b</sup>	1.6	0.9	1.0	4.4	1.3	2.9	2.1
MP2/BS1 <sup>b</sup>	0.9	1.6	1.0	2.5	1.3	1.5	1.5
MP2/BS2 <sup>b</sup>	0.2	0.0	0.0	0.0	0.0	0.0	0.0

<sup>a</sup> Mean value of the percent difference compared to CCSD(T)/BS4 (for **1** and **2**), MP2/BS2 (for **3-6** and **10**) and mPW1PW91/BS2 (for **7**, **8** and **11**). <sup>b</sup> Mean value of the percentage difference compared to CCSD(T)/BS4 (for **1** and **2**) and MP2/BS2 (for **3-6** and **10**).

**Table 3.** Comparison of the relative energy (in kJ/mol) of **1-11** with various methods.

Method <sup>a</sup>	PM3	HF		BP86	B3LYP		mPW1PW91		MPW1K	MP2		CCSD(T)			
Basis set <sup>a</sup>		BS1	BS2	BS1	BS1	BS2	BS1	BS2	BS1	BS1	BS2	BS1	BS2	BS3	BS4
Single-point relative energies obtained at the CCSD(T)/BS4 level compared to CCSD(T)/BS4//CCSD(T)/BS4															
<b>1</b>	7.8	1.6	2.7	2.3	0.5	0.5	0.1	0.2	0.0	0.7	0.1	0.7	0.4	0.1	0.0
<b>2</b>	1.2	1.7	5.1	2.3	1.5	0.3	0.3	0.1	0.1	0.6	0.0	2.2	0.2	0.1	0.0
Single-point relative energies obtained at the CCSD(T)/BS3 level compared to CCSD(T)/BS3//MP2/BS2															
<b>3</b>	26.6	2.8	5.4	7.1	2.1	0.7	1.8	-0.5	1.4	3.1	0.0				
<b>4</b>	20.2	7.0	7.0	20.6	13.1	1.0	13.4	0.0	11.8	11.9	0.0				
<b>5A</b>	39.0	4.1	8.9	9.7	2.7	0.9	2.4	-0.3	1.7	3.7	0.0				
<b>5B</b>	35.4	3.9	7.4	8.5	2.4	0.7	2.4	-0.7	2.5	3.4	0.0				
<b>6</b>	34.7	7.0	10.2	21.3	9.8	1.2	10.6	0.3	8.6	8.2	0.0				
<b>10</b>	12.3	2.3	3.5	5.1	1.4	0.3	1.6	-0.4	1.6	2.9	0.0				
Single-point relative energies obtained at the MP2/BS3 level compared to MP2/BS3//mPW1PW91/BS2															
<b>7</b>	62.6	18.1			-1.3			-1.0	0.0						
<b>8</b>	49.6	19.1			0.0			1.2	0.0						
<b>11</b>	50.0	17.1			-2.3			-1.4	0.0						
Mean values															
<sup>b</sup>	22.2	3.8	6.3	9.6	4.2	0.7	4.1	-0.2	3.5	4.3	0.0				
<sup>c</sup>	30.9	7.7			2.7			2.9	-0.1						

<sup>a</sup> method and basis set used for geometry optimization. <sup>b</sup> mean value based on results for **1-6** and **10**. <sup>c</sup> mean value based on results for **1-11**.

**Table 4.** Relative stability (in kJ/mol) of **5A** versus **5B** obtained at various levels of calculation<sup>a</sup>.

Method <sup>b</sup>	PM3	HF		BP86	B3LYP		mPW1PW91		MPW1K	MP2	
		BS1	BS2	BS1	BS1	BS2	BS1	BS2	BS1	BS1	BS2
Opt <sup>c</sup>	45	2	11	23	18	28	8	19	13	11	19
B3LYP/BS1 <sup>d</sup>	17	16	16	17	18	19	18	18	18	17	18
B3LYP/BS2 <sup>d</sup>	25	28	26	28	29	28	29	28	30	29	28
B3LYP/BS3 <sup>d</sup>	25	28	26	28	29	27	29	28	30	29	28
MP2/BS1 <sup>d</sup>	10	10	10	9	10	12	10	10	11	11	11
MP2/BS2 <sup>d</sup>	15	19	18	18	19	19	20	19	20	19	19
MP2/BS3 <sup>d</sup>	16	20	19	20	21	20	21	20	22	21	20
CCSD(T)/BS1 <sup>d</sup>	8	8	8	6	8	9	7	8	8	8	8
CCSD(T)/BS2 <sup>d</sup>	14	16	15	15	16	16	16	16	17	16	16
CCSD(T)/BS3 <sup>d</sup>	14	18	17	17	18	18	18	18	19	18	18

<sup>a</sup> a positive value indicates that **5A** is lower in energy than **5B**. <sup>b</sup> method and basis set used for geometry optimization. <sup>c</sup> relative stability at the level used for geometry optimisation. <sup>d</sup> method and basis set used for single-point energy calculation.

**Table 5.** Protonation energy (in kJ/mol) of zinc-bound hydroxide obtained at the level of optimization.

Method	PM3	HF		BP86	B3LYP		mPW1PW91		MPW1K	MP2		CCSD(T)			
Basis set		BS1	BS2	BS1	BS1	BS2	BS1	BS2	BS1	BS1	BS2	BS1	BS2	BS3	BS4
<b>2</b>	202	413	380	280	299	264	322	286	350	349	301	352	308	293	291
<b>4</b>	566	726	699	697	705	659	708	667	713	709	664				
<b>6</b>	619	741	721	708	717	683	719	689	723	719	686				
<b>8</b>	727	853			832		834	803							

**Table 6.** Protonation energy (in kJ/mol) of zinc-bound hydroxide of **2** obtained at various levels of calculation.

Method <sup>a</sup>	PM3	HF		BP86	B3LYP		mPW1PW91		MPW1K	MP2		CCSD(T)			
		BS1	BS2	BS1	BS1	BS2	BS1	BS2	BS1	BS1	BS2	BS1	BS2	BS3	BS4
B3LYP/BS1 <sup>b</sup>	296	301	306	298	299	299	299	300	300	299	300	299	299	299	300
B3LYP/BS2 <sup>b</sup>	258	264	266	263	264	264	263	264	263	263	264	264	263	263	263
B3LYP/BS3 <sup>b</sup>	252	256	259	256	257	256	256	256	256	255	256	257	256	256	256
MP2/BS1 <sup>b</sup>	339	350	354	347	349	348	349	349	349	349	349	350	348	348	349
MP2/BS2 <sup>b</sup>	294	302	304	301	302	301	301	301	301	301	301	303	301	301	301
MP2/BS3 <sup>b</sup>	278	285	287	284	286	284	284	284	284	284	284	286	284	284	284
MP2/BS4 <sup>b</sup>	274	281	283	282	283	281	282	281	281	282	281	284	281	281	281
CCSD(T)/BS1 <sup>b</sup>	344	354	358	350	352	352	352	353	353	352	353	352	352	352	353
CCSD(T)/BS2 <sup>b</sup>	303	309	312	307	308	308	308	308	308	308	308	309	308	308	308
CCSD(T)/BS3 <sup>b</sup>	288	294	297	292	293	293	293	293	293	292	293	294	293	293	293
CCSD(T)/BS4 <sup>b</sup>	284	291	293	291	292	291	291	291	291	291	291	292	291	291	291

<sup>a</sup> method and basis set used for geometry optimization. <sup>b</sup> method and basis set used for single-point energy calculation.

**Table 7.** Metal-water bond dissociation energy<sup>b</sup> (in kJ/mol) computed at the level of geometry optimization.

Method <sup>a</sup>	PM3	HF		BP86	B3LYP		mPW1PW91		MPW1K	MP2		CCSD(T)				
Basis set <sup>a</sup>		BS1	BS2	BS1	BS1	BS2	BS1	BS2	BS1	BS1	BS2	BS1	BS2	BS3	BS4	
<b>1</b>	E <sub>prep</sub>	3	3	3	4	4	4	4	4	3	3	4	3	4	3	3
	E <sub>int</sub>	287	371	371	447	442	437	426	428	416	406	404	399	401	401	411
	BSSE	-	9	5	15	15	6	11	6	11	16	14	15	14	6	4
	E <sub>bond</sub> <sup>c</sup>	284	359	364	427	423	427	412	418	402	387	387	382	384	391	404
<b>3</b>	E <sub>prep</sub>	21	24	21	22	23	23	23	22	23	24	22				
	E <sub>int</sub>	114	177	165	161	170	160	171	164	177	179	170				
	BSSE	-	13	5	22	22	6	20	6	18	24	17				
	E <sub>bond</sub> <sup>c</sup>	93	140	138	117	125	132	129	136	136	131	131				
<b>5B</b>	E <sub>prep</sub>	3	25	26	19	20	24	14	18	22	22	24				
	E <sub>int</sub>	20	130	110	124	130	103	130	107	134	135	115				
	BSSE	-	15	5	27	25	5	23	6	20	26	15				
	E <sub>bond</sub> <sup>c</sup>	16	90	79	78	84	74	95	84	91	87	76				
<b>7</b>	E <sub>prep</sub>	19	22			20		20	22							
	E <sub>int</sub>	67	135			129		131	121							
	BSSE	-	16			26		23	7							
	E <sub>bond</sub> <sup>c</sup>	48	98			83		88	92							

<sup>a</sup> method and basis set used for geometry optimization. <sup>b</sup> preparation energy E<sub>prep</sub> : energy difference between the two optimized fragments (H<sub>2</sub>O, and **9**, **10**, **3**, **11**) and the fragments in their geometries within the complex (**1**, **3**, **5B**, **7** respectively); Interaction

energy  $E_{\text{int}}$  : energy difference between the optimized complex (**1**, **3**, **5B**, **7**) and the fragments in their geometries within the complex;  
Bond dissociation energy corrected for BSSE  $E_{\text{bond}}^{\text{c}}$  : energy difference between the optimized complex (**1**, **3**, **5B**, **7**) and the two optimized fragments ( $\text{H}_2\text{O}$ , and **9**, **10**, **3**, **11** respectively) including basis set superposition error (BSSE) for *ab initio* and DFT methods (see Figure 5).

**Table 8.** Metal-water bond dissociation energy  $E_{\text{bond}}$  (in kJ/mol) of **1** obtained at various levels of calculation.

Method <sup>a</sup>	PM3	HF		BP86	B3LYP		mPW1PW91		MPW1K	MP2		CCSD(T)			
Basis set <sup>a</sup>		BS1	BS2	BS1	BS1	BS2	BS1	BS2	BS1	BS1	BS2	BS1	BS2	BS3	BS4
B3LYP/BS1 <sup>b</sup>	434	438	438	438	438	438	438	438	438	438	438	438	438	438	438
B3LYP/BS2 <sup>b</sup>	428	432	432	433	432	433	433	433	432	433	433	433	433	433	433
B3LYP/BS3 <sup>b</sup>	426	429	429	430	429	430	430	430	430	430	430	430	430	430	430
MP2/BS1 <sup>b</sup>	393	402	402	401	403	403	403	402	403	403	403	403	402	402	403
MP2/BS2 <sup>b</sup>	394	400	400	400	400	401	401	401	401	401	401	401	401	401	401
MP2/BS3 <sup>b</sup>	394	400	400	400	400	400	400	400	400	400	400	400	400	400	401
MP2/BS4 <sup>b</sup>	402	409	409	409	410	410	410	409	410	410	410	410	410	410	410
CCSD(T)/BS1 <sup>b</sup>	388	397	397	395	397	397	397	397	397	397	397	397	397	397	397
CCSD(T)/BS2 <sup>b</sup>	392	398	398	396	397	397	397	397	397	397	397	397	397	397	397
CCSD(T)/BS3 <sup>b</sup>	392	397	397	397	397	397	397	397	397	397	397	397	397	398	397
CCSD(T)/BS4 <sup>b</sup>	401	407	407	407	407	408	407	407	408	408	408	407	407	408	408

<sup>a</sup> method and basis set used for geometry optimization. <sup>b</sup> method and basis set used for single-point energy calculation.

**Table 9.** First-second shell interaction energy<sup>b</sup> (in kJ/mol) obtained at the level of geometry optimization.

Method <sup>a</sup>	PM3	HF		BP86	B3LYP		mPW1PW91		MPW1K	MP2		
Basis set <sup>a</sup>		BS1	BS2	BS1	BS1	BS2	BS1	BS2	BS1	BS1	BS2	
<b>5A</b>	E <sub>prep</sub>	2	8	7	12	10	10	11	11	11	10	9
	E <sub>int</sub>	64	115	102	140	138	117	137	119	135	134	119
	BSSE	-	6	4	12	12	5	10	6	9	13	12
	E <sub>bond</sub> <sup>c</sup>	62	101	91	116	116	101	116	103	116	112	97
<b>6</b>	E <sub>prep</sub>	3	12	7	35	26	12	27	14	24	21	11
	E <sub>int</sub>	11	104	81	151	141	96	143	102	138	135	100
	BSSE	-	16	4	33	31	6	27	6	22	33	15
	E <sub>bond</sub> <sup>c</sup>	9	76	68	84	84	77	88	80	92	81	73

<sup>a</sup> method and basis set used for geometry optimization. <sup>b</sup> preparation energy E<sub>prep</sub> : energy difference between the two optimized fragments (H<sub>2</sub>O, and **3** or **4**) and the fragments in their geometries within the complex (**5A** or **6** respectively); Interaction energy E<sub>int</sub> : energy difference between the optimized complex (**5A** or **6**) and the fragments in their geometries within the complex; Bond dissociation energy corrected for BSSE E<sub>bond</sub><sup>c</sup> : energy difference between the optimized complex (**5A** or **6**) and the two optimized fragments (H<sub>2</sub>O, and **3** or **4** respectively) including basis set superposition error (BSSE) for *ab initio* and DFT methods (see figure 5).

**Table 10.** complex-second shell water bond dissociation energy  $E_{\text{bond}}$  of **5A** (in kJ/mol) obtained at various levels of calculation.

Method <sup>a</sup>	PM3	HF		BP86	B3LYP		mPW1PW91		MPW1K	MP2	
Basis set <sup>a</sup>		BS1	BS2	BS1	BS1	BS2	BS1	BS2	BS1	BS1	BS2
B3LYP/BS1 <sup>b</sup>	114	125	124	127	128	127	128	127	128	127	127
B3LYP/BS2 <sup>b</sup>	98	106	105	106	107	107	106	107	106	107	107
B3LYP/BS3 <sup>b</sup>	92	100	100	101	101	102	101	101	101	101	102
MP2/BS1 <sup>b</sup>	111	123	122	123	124	124	124	124	124	124	124
MP2/BS2 <sup>b</sup>	100	109	108	109	110	110	109	110	109	110	110
MP2/BS3 <sup>b</sup>	94	105	104	105	106	106	106	106	106	106	106
CCSD(T)/BS1 <sup>b</sup>	109	121	120	120	121	121	121	121	121	121	121
CCSD(T)/BS2 <sup>b</sup>	100	108	108	108	109	109	108	109	108	109	109
CCSD(T)/BS3 <sup>b</sup>	94	105	104	105	105	105	105	105	105	105	105

<sup>a</sup> method and basis set used for geometry optimization. <sup>b</sup> method and basis set used for single-point energy calculation.

**Table 11.** Main geometrical parameters (d, in Å) obtained for complexes **12-14** and relative differences ( $\Delta$ ) from the experimental geometry with various methods.

Method	PM3		HF		B3LYP		MPW1PW91		Exp. <sup>a</sup>
Basis set			BS1'		BS1'		BS2'		
	d	$\Delta$	d	$\Delta$	d	$\Delta$	d	$\Delta$	
<b>12</b>									
Zn-O	2.165	0.193	1.969	-0.003	1.940	-0.032	1.948	-0.024	1.972
Zn-N <sup>b</sup>	2.020	0.024	2.058	0.062	2.014	0.018	2.031	0.035	1.996
ZnO $\cdots$ OH <sub>2</sub>	2.671	0.132	2.631	0.092	2.548	0.009	2.516	-0.023	2.539
ZnO $\cdots$ O	2.759	-0.063	2.787	-0.035	2.771	-0.051	2.711	-0.111	2.822
H <sub>2</sub> O $\cdots$ O	2.690	-0.330	3.111	0.091	2.851	-0.169	2.779	-0.241	3.020
OH <sub>2</sub> $\cdots$ X <sup>c</sup>	3.453	0.205	3.330	0.082	3.212	-0.036	3.236	-0.012	3.248
Mean value <sup>d</sup>		0.158		0.061		0.052		0.074	
<b>13</b>									
Zn-O	2.221		2.025		1.999		2.009		
Zn-N <sup>b</sup>	2.015		2.049		2.009		2.019		
ZnO $\cdots$ O <sup>b</sup>	3.195		2.991		2.860		2.877		
<b>14</b>									
Zn-O	1.953		1.818		1.824		e		
Zn-N <sup>b</sup>	2.044		2.106		2.063		e		

<sup>a</sup> selected experimental parameters[Sénèque, 2001 #25] <sup>b</sup> mean value. <sup>c</sup> center of the phenyl ring of the OH/ $\pi$  interaction. <sup>d</sup> average of the absolute value of the relative differences from the experimental geometry of **12** <sup>e</sup> geometry optimization not carried out at this level.

**Table 12.** relative Zn-O and O··O bond lengths variation (in Å) obtained with various methods.

bond	Entry	Method/basis set	PM3	HF/BS1 <sup>a</sup>	B3LYP/BS1 <sup>a</sup>	MPW1PW91/BS2 <sup>a</sup>
Zn-O	1	<b>7-8</b>	+0.312	+0.300	+0.296	+0.255
	2	<b>13-14</b>	+0.268	+0.207	+0.175	
	3	<b>8-14</b>	-0.044	+0.014	+0.011	
	4	<b>7-13</b>	0.000	+0.107	+0.132	
	5	<b>3-5A</b>	+0.027	+0.053	+0.064	
	6	<b>13-12</b>	+0.056	+0.056	+0.059	+0.061
O··O	7	<b>5A-12</b>	+0.021	+0.111	+0.124	+0.111

<sup>a</sup> BS1' for **12-14** and BS2' for **12-13**.

**Table 13.** Relative energy, protonation energy and first-second shell interaction energy (in kJ/mol) obtained at various levels of calculation for **12-14**.

Compounds	Method/basis set	optimization			
		PM3	HF/BS1	B3LYP/BS1	MPW1PW91/BS2
Single-point calculation					
Single-point relative energy					
<b>12</b>	B3LYP/BS2	+163.7	+35.3	0.0	-5.6
	B3LYP/BS3'	+169.1	+40.5	0.0	-4.6
<b>13</b>	B3LYP/BS2	+159.5	+31.6	0.0	-3.9
	B3LYP/BS3'	+162.3	+35.2	0.0	-5.2
<b>14</b>	B3LYP/BS2	+127.1	+37.8	0.0	
	B3LYP/BS3'	+134.3	+42.0	0.0	
Protonation energy					
<b>14</b>	B3LYP/BS2	908	946	940	
	B3LYP/BS3'	920	955	948	
First-second shell interaction energy					
<b>12</b>	B3LYP/BS2	61.1	61.8	64.6	66.1
	B3LYP/BS3'	58.8	60.4	65.2	64.3